

T-2079

PROPERTIES OF HIGH QUALITY FOAM CEMENT

by

James S. Lebsack

ARTHUR LAKES LIBRARY
COLORADO SCHOOL of MINES
GOLDEN, COLORADO 80401
CLOSED RESERVE

ProQuest Number: 11016484

All rights reserved

INFORMATION TO ALL USERS

The quality of this reproduction is dependent upon the quality of the copy submitted.

In the unlikely event that the author did not send a complete manuscript and there are missing pages, these will be noted. Also, if material had to be removed, a note will indicate the deletion.



ProQuest 11016484

Published by ProQuest LLC (2019). Copyright of the Dissertation is held by the Author.

All rights reserved.

This work is protected against unauthorized copying under Title 17, United States Code
Microform Edition © ProQuest LLC.

ProQuest LLC.
789 East Eisenhower Parkway
P.O. Box 1346
Ann Arbor, MI 48106 – 1346

A Thesis submitted to the Faculty and the Board of Trustees of the Colorado School of Mines in partial fulfillment of the requirements for the degree of Master of Science in Petroleum Engineering.

Signed: James S. Lebsack
Student

Golden, Colorado

Date: May 22, 1978

Approved: L. M. Barr
Thesis Advisor

L. M. Barr
Head of Department

Golden, Colorado

Date: May 22, 1978

ABSTRACT

Laboratory tests were conducted with samples of foamed Class G oil-well cement. These tests were conducted on cement slurries and samples of set cement with air volumes between 50 and 90% of the total volume of the sample.

Samples of set cement were tested for permeability, porosity, pore size and pore size distribution. Cement slurries were pressed against a sandpack with differential pressures of five, ten and twenty-five psi. Additional tests were conducted with a standard A.P.I. low pressure-low temperature filter press.

Permeabilities were found to increase dramatically with increased air concentrations. Reported values range from 26 millidarcies to 21 darcys for samples containing 48 to 77% air.

Total pore volume was found to be consistently higher than the air volume of the sample. This pore volume is interconnected; however, a large number of "dead end" pores exist.

Pore size increased with air concentration and had a much wider distribution than graded 20-40 mesh sand. This data indicated that the foam is not totally stable over the cement setting time and that more concentrated foams are less stable.

Foamed cement slurries containing approximately 70% air were pressed against 20-40 mesh sand. The cement did not enter the sand while the majority of the air was lost. Filter press data indicated that the water loss is independent of the air concentration; however, the spurt loss is decreased with increasing air concentration.

TABLE OF CONTENTS

ABSTRACT	iii
TABLE OF CONTENTS	v
LIST OF FIGURES	vii
LIST OF TABLES	ix
INTRODUCTION	1
LITERATURE SURVEY	3
Portland Cement	3
Foams	5
Cellular Concrete	8
THEORETICAL DEVELOPMENT	11
Permeability of Foam Cement	11
Pore Size Distribution	13
DISCUSSION OF EXPERIMENT	16
Sample Preparation	16
Foam Quality	19
Measurement of Permeability	20
Total and Displaced Porosity	23
Pore Size Distribution	24
Foam Cement with Unconsolidated Sand	25
Filter Loss of Foam Cement	26
DISCUSSION OF RESULTS	28
Hardened Foam Cement	28
Foam Cement Slurries	32

Effect of Experimental Procedures	33
Recommendations for Further Study	34
CONCLUSIONS	36
FIGURES	37 - 69
TABLES	70 -114
BIBLIOGRAPHY	115
APPENDICES	118 -122

LIST OF FIGURES

1.	Surface Tension of Adofoam BF-1 in Tap Water	37
2.	Predicted and Measured Qualities	38
3	Permeability of Foam Cement	39
4.	Total Porosity of Foam Cement	40
5.	Displaced Porosity of Foam Cement	41
6.	Initial Water Saturation of Foam Cement	42
7.	Median Pore Size of Foam Cement	43
8.	Water Loss of Foam Cement	44
9.	Flow Rate Versus Pressure, Sample 1	45
10.	Flow Rate Versus Pressure, Sample 2	46
11.	Flow Rate Versus Pressure, Sample 3	47
12.	Flow Rate Versus Pressure, Sample 4	48
13.	Flow Rate Versus Pressure, Sample 5	49
14.	Flow Rate Versus Pressure, Sample 6	50
15.	Flow Rate Versus Pressure, Sample 7	51
16.	Flow Rate Versus Pressure, Sample 8	52
17.	Flow Rate Versus Pressure, Sample 9	53
18.	Flow Rate Versus Pressure, Sample 10	54
19.	Flow Rate Versus Pressure, Sample 13	55
20.	Flow Rate Versus Pressure, 20-40 Mesh Sand	56
21.	Pore Size Distribution, Sample 1	57
22.	Pore Size Distribution, Sample 2	58
23.	Pore Size Distribution, Sample 3	59
24.	Pore Size Distribution, Sample 4	60

25.	Pore Size Distribution, Sample 5	61
26.	Pore Size Distribution, Sample 6	62
27.	Pore Size Distribution, Sample 7	63
28.	Pore Size Distribution, Sample 8	64
29.	Pore Size Distribution, Sample 9	65
30.	Pore Size Distribution, Sample 10	66
31.	Pore Size Distribution, 20-40 Mesh Sand	67
32.	Miscible Displacement in Laminar and Turbulent Flow, Sample 2	68
33.	Schematic Diagram of Test Apparatus	69

LIST OF TABLES

1.	Surface Tension of Adofoam BF-1 in Tap Water	70
2.	Properties of Class G Cement	71
3.	Test Data, Samples 1 thru 13	72
thru 15.		
16.	Test Data, 20-40 Mesh Sand	78
17.	Filter Loss of Foam Cement	79
18.	Interaction of Foam Cement with 20-40 Mesh Sand	80
19.	Pressure Versus Flow Rate, Samples 1 thru 10	81
thru 28.		
29.	Pressure Versus Flow Rate, Sample 13	91
30.	Pressure Versus Flow Rate, 20-40 Mesh Sand	92
31.	Pore Size Distribution, Sample 1 thru 10	93
thru 40.		
41.	Pore Size Distribution, 20-40 Mesh Sand	112
42.	Miscible Displacement in Turbulent Flow Regime, Sample 2	113

INTRODUCTION

Foam cement is a mixture of dry cement, water, gas and a suitable surface active agent. With sufficient shearing, these basic components yield an aggregation of gas bubbles separated from one another by thin films of cement slurry. The continuous cement phase hardens to form a solid skeleton about the dispersed gas phase.

The gas bubbles may or may not be interconnected in the set cement, depending largely on the foam quality of the slurry. Quality is a property of the slurry and is defined as the ratio of the gas volume to the total volume of all the components. The quality of the slurry is dependent on the pressure and temperature and will vary slightly from that of the set cement due to shrinkage and hydration.

Foamed concretes have been used in the construction industry for many years^{1,2}. Generic descriptions include cellular, porous, aerated and gaseous concrete. The primary advantages of these concretes are reduced material cost, low density and low thermal conductivity.

The application of foam cement to problems associated with oil and gas production has great potential. Benefits could be derived from permeable or impermeable foam cements.

Impermeable foam cement could supplement or replace

current cementing practice with savings in material and handling cost. Lost circulation in underpressured areas would decrease due to the lighter weight of foam cement. The thermal properties of foam cement could be advantageous in permafrost, steamfloods or areas where paraffin deposition is a problem.

Highly permeable foam cement may find application in sand consolidation or as a proppant for hydraulic fractures. Water base foams have been successful in fracturing shallow formations and foam cement may be a logical extension of this practice. Russian literature³ indicates that foam cement has been field tested and "classified successful" in "consolidation of the well bottom zone".

This investigation was conducted for the specific application of foam cement to sand consolidation. Qualities were varied from 50 to 90% and studied for permeability, porosity, pore size and pore size distribution. The interaction of foam cement slurries with unconsolidated sand was also investigated.

LITERATURE SURVEY

Published literature which is pertinent to this investigation can be classified into the following three categories:

1. Portland cements
2. Foams
3. Cellular concrete

Each of these items have specific properties which yield insight into the purpose of this study as well as an understanding of the results which were obtained.

PORTLAND CEMENT

The initial patent for portland cement was granted in 1824 to Joseph Aspdin⁴. This product was manufactured by burning a blend of limestone and clay. Subsequent addition of water to this blend set it into a hardened mass. Many refinements have been made in the manufacture of portland cements so that specific blends are now available for a diverse range of applications.

Modern portland cements have four basic chemical components^{5,6}. Tricalcium silicate is the prevalent compound and the major contributor to strength, particularly in the early setting stage. Dicalcium silicate hydrates slowly and produces additional long term strength. Tricalcium

aluminate hydrates rapidly and is used to control the initial set and thickening time of the cement. Tetra-calcium aluminoferrite has little effect on the properties of the set cement but does affect the hydration of the tricalcium aluminate.

Specifications for oil well cements were set in 1961 by the American Petroleum Institute⁷. API Class G cement was used in this study because of its composition and availability. The recommended water to cement mixing ratio is 0.44 (by weight) which results in a slurry density of 15.8 pounds per gallon.

Class G cement is similar in composition to API Class B, Class H and ASTM C 150 type II cements. It is manufactured to rigorous physical and chemical specifications, has a high resistance to sulfate attack and is compatible with all oil well cement additives currently in use. Class G and Class H cements are readily available in all regions where foam cement might be applied.

Cement slurries normally have a high water loss in relation to drilling fluids. A.P.I. low pressure-low temperature filter loss tests are conducted at room temperature and 100 psi, with results reported in cc's of effluent over a 30 minute interval. It has been noted that cement will dehydrate in as little as 40 seconds under these test conditions. A number of additives are commercially available

to reduce water loss; however, these agents generally retard the set and thickening time of the cement.

The permeability of set cement is typically less than 0.1 millidarcy although values as high as 16 millidarcies have been reported⁹. All properties of cement are effected by moisture content and the reported values of permeability were obtained from dry samples of cement. Lower values would be expected from moist samples.

FOAMS

A foam is a coarse dispersion of gas in liquid with the discontinuous gas phase separated by thin films of the continuous liquid phase¹⁰. Dilute foams are characterized by spherical gas bubbles and thick liquid films while the concentrated foams consist of polyhedral gas cells separated by thin liquid films¹¹.

Thermodynamically all foam systems are unstable. Pure liquids form only transitory foams, with stable life normally less than one second. A high degree of stability can be obtained with the addition of a surface active agent. A fourth phase consisting of solid particles has also been found to stabilize certain foams¹³. Factors which effect foam stability include the rate of liquid drainage, film rupture followed by coalescence, the size and distribution of the gas bubbles, the surface transport mechanism of the surface

active agent, film elasticity and electrical properties of the foam.

Liquid drainage occurs because of gravitational and capillary pressure forces. A properly chosen surfactant will increase the surface and bulk viscosity of the fluid, thereby retarding the drainage rate of the fluid. Continued drainage will reduce the film thickness to a point where molecular attractive forces cause the film to rupture..

The internal pressure of an individual gas bubble is inversely proportional to the radius of the bubble. The rate of gas diffusion between bubbles is therefore dependent on their relative size, as well as the thickness and permeability of the liquid film.

Anionic and cationic surface active agents provide a small degree of stability because of electrical repulsion. These agents create an electric double layer at the gas-liquid interface. As film thinning takes place, the two bubbles are drawn closer and the like charges of the two electric double layers repel one another. This will retard the continued thinning of the liquid film but does not effect the initial rate of liquid drainage.

The subject of foam stability is complex and involves a number of interrelated factors. Tests to determine the stability of a foam are qualitative in nature and tend to focus on only one aspect of foam stability, such as the

liquid drainage rate or the viscosity of the foam.

Water based foams have been widely applied in the petroleum industry. Drilling and workover operations benefit from the low density of foam^{14,15}, while formation fracturing with foam has several benefits¹⁶. Laboratory investigations have also been conducted for the use of foams in enhanced oil recovery^{17,18}.

Hutchinson¹⁴ and Abbott¹⁹ have reported that foams have an excellent carrying capacity. Abbott studied the slip velocities of spherical particles in flowing foam while Hutchinson reported that three inch particles were carried by foam in normal field operations.

Blauer and Kohlhaas¹⁶ reported that the settling velocity of small-diameter particles in static foam is much less than predicted by Stokes' Law. This difference became larger as the particle size decreased and it was surmised that particles smaller than the gas bubbles were retained in the foam structure.

Results of fluid loss tests conducted with sandpacks of 2000, 500, and 170 millidarcies were also reported by Blauer and Kohlhaas. Their data shows a significant increase in fluid loss with permeability and that a 70% foam quality had nearly five times the loss of an 80% quality foam.

King²⁰ studied the water loss of foam under dynamic conditions. Measurements were made on sandstone wafers 0.2

inches thick with permeabilities less than one millidarcy. He reported that water loss increased with increased differential pressure and permeability but was independent of quality between 70 and 90%.

King also noted the existence of foam in the effluent when core wafers with permeability higher than one millidarcy were tested. The percentage of foam in the effluent increased with higher permeability. The foam may pass through the wafer as a body or be regenerated due to higher velocities.

CELLULAR CONCRETE

The use of powdered metals as gas-forming agents in concrete was patented in 1914 by Aylsworth and Dyer²⁴. A typical process involved the mixing of powdered aluminum with the dry cement and sodium hydroxide in the mix water. The reaction of one pound of aluminum with sodium hydroxide released twenty cubic feet of hydrogen at standard conditions. A very homogenous mixture can be attained with this process but it is costly and of little value at the pressures encountered in potential petroleum applications.

Bayer²⁵ was granted several patents beginning in 1923 for the use of preformed foams mixed with the concrete slurry. Additional refinements in the preparation of cellular concrete were extensively reviewed by Valore¹.

Valore described two methods of preparing foam cement. The "mix-foam" method involves the addition of a surface active agent to the mixed cement slurry followed by agitation in the presence of air. The "pre-foam" method described by Bayer was found to have two major advantages over the mix-foam process. The surfactant requirement in the pre-foam process was typically 10% of that required in the mix-foam method. Prediction of the quality was enhanced due to a close relationship between the input volume of foam and the air content of the set cement.

Aldrich²¹ employed the mix-foam method in a batch process. He reported that the quality obtained was dependent on the mixing time and the concentration of surfactant. Slattery²² and Al-Mashat²³ each employed continuous mixing processes in which nitrogen was injected into a slurry of cement and surfactant. Slattery reported that the quality could not be predetermined, even though he was working with a closed system. This may have been due to the problems which he encountered with gas surging and the resulting imbalance in the mix components. Al-Mashat apparently did not encounter these problems.

Aldrich studied the porosity and permeability of foam cement. He found that the porosity of the set sample was lower than the slurry quality. This difference was attributed to shrinkage of the pores and the solid cement when the sample

was dehydrated. Permeability was measured with gas on dry samples of foam cement. Reported values of permeability were less than 0.28 millidarcies (the minimum detectable) below a quality of 43.5%. Permeability increased rapidly above a quality of 47.5% to several darcies at 53%.

Additional studies conducted by Aldrich²⁶ found that high quality foam cement would enter a sandpack and retain a high permeability. The precise quality of the cement and the sand size which were used was not reported. It was noted that no stress (differential pressure) was applied to the slurry.

Suleimanof³ conducted field trials with foam cement for the purpose of "consolidating the well bottom zone". Six wells were treated with foam cement of approximately 30% quality. The method of placement is not clear; however, it was reported that the producing interval was washed or drilled out after treatment. Five of the wells showed an increase in production after treatment while the period between well overhauls was increased in all six wells.

THEORETICAL DEVELOPMENTPERMEABILITY OF FOAM CEMENT

The attainment of high permeability in foam cement is due to interference between the individual gas bubbles. The minimum quality at which interference can occur is in cubic packing of equal size spheres. The bulk volume of foam cement occupied by one gas bubble is

$$V_b = (2R)^3 \quad (1)$$

If the film thickness is ignored, the volume occupied by the gas is

$$V_g = \frac{4}{3} \pi R^3 \quad (2)$$

Dividing the gas volume (eq. 2) by the total volume (eq. 1) yields the fractional quality at which interference begins.

$$\text{Quality} = \frac{\pi}{6} = 52.36\% \quad (3)$$

It may be noted that this quality is not a function of the number or diameter of the spheres, providing they are of equal size. A further increase in gas concentration will

initially change the packing geometry, followed by the deformation of the spheres into polyhedrans.

Permeability develops from the breakage of the solid cement film. The film must solidify before breaking or the foam structure would simply collapse. Applying the theory of elasticity to a thick walled sphere, the tangential stress is

$$S_t = \frac{P_o b^3 (2R^3 + a^3)}{2R^3 (a^3 - b^3)} - \frac{P_i a^3 (2R^3 + b^3)}{2R^3 (a^3 - b^3)} \quad (5)$$

Where: S_t = Tangential Stress (+ = tension)

P_i = Internal Pressure

P_o = External Pressure

a = Internal Radius

b = External Radius

R = Radius at Point of Stress

If the effects of gas diffusion and heat of hydration are ignored, the internal pressure of the gas bubble can be related to the surface tension (σ) of the liquid and the external pressure

$$P_i = P_o + \frac{2\sigma}{R} \quad (5)$$

Substituting equation 5 into equation 4 and rearranging

terms, the tangential stress is

$$S_t = \frac{\sigma a^3 (2R^3 + b^3)}{R^4 (b^3 - a^3)} - P_o \quad (6)$$

Evaluation of equation 6 at the boundaries yields the following stress equations

$$@ R = a: \quad S_t = \frac{\sigma (2a^3 + b^3)}{a (b^3 - a^3)} - P_o \quad (7)$$

$$@ R = b: \quad S_t = \frac{3 \sigma a^3}{b (b^3 - a^3)} - P_o \quad (8)$$

Similar calculations can be made for the radial stress at the internal and external boundary which yield the internal pressure and external pressure, respectively.

It should be noted that the maximum tensile stress is attained at the minimum wall thickness. This minimum film thickness is attained in foam cement when bubble interference occurs.

PORE SIZE DISTRIBUTION

The measurement of pore size distribution is an attempt to characterize the geometry of the flow channels in porous media. The method employed in this investigation was first presented by Klinkenberg²⁷ and assumes that the porous media

can be represented by an assemblage of straight cylindrical capillaries.

When the sample is saturated with distilled water and displaced by a dilute solution of NaCl, the amount of distilled water produced in the effluent should approach the effective pore volume of the sample. This could be accomplished with any miscible fluids; however, the use of water simplifies calculations because variations in density and viscosity are negligible.

The maximum capillary radius can be determined when the initial trace of salt solution appears in the effluent.

$$r_x = \left\{ \frac{8 K V_b}{V} \right\}^{\frac{1}{2}} \quad (9)$$

Where: r_x = Equivalent Capillary Radius
 K = Permeability of Sample
 V_b = Bulk Volume of Sample
 V = Injection Volume

Equation 9 is obtained from the combination of Poiseuille's Law (capillary tubes) with Darcy's Law (porous media) and is subject to the same assumptions and restrictions.

Calculation of r_x as displacement continues yields the cumulative pore size distribution. The fraction of the pore volume occupied by tubes of radius r_x to r_{max} can be determined

as follows:

$$S = \frac{R - V \cdot \frac{dR}{dV}}{V_p} \quad (10)$$

Where: S = Fraction of Pore Volume Occupied by

Capillaries of Radius r_x to r_{max}

R = Volume of Displaced Phase in Effluent

V_p = Effective Pore Volume

$\frac{dR}{dV}$ = Fraction of Displaced Phase in Effluent

Detailed derivations of equations 9 and 10 can be found in the cited reference.

DISCUSSION OF EXPERIMENT

In this section, the experimental procedure is discussed and the experimental results are presented.

SAMPLE PREPARATION

Three types of mixing procedures were attempted in the course of this work. Batch mixing of all components would generally not yield the high qualities necessary to this study. A continuous mixing system similar to that employed by Slattery was found to be unworkable. Batch mixing of a preformed foam with the cement slurry yielded a consistent and predictable high quality foam cement.

Batch mixing of all components was attempted with the use of a standard Waring blender. The surfactant was mixed with water followed by the addition of dry cement. These components were mixed with a stirring rod until a consistent slurry was obtained. The slurry was then mixed in a high speed blender (6,000-8,000 RPM) in an effort to foam the mixture. A high degree of vertical segregation was noted in the mixture. In addition, the mixture would thicken and reduce air entrainment prior to obtaining the desired quality. Sample number one was obtained with this procedure.

Persistent problems with gas surging were encountered with a continuous mixing system. This problem was because

of the low pressures and small volumes required by this study. The gas metering systems available simply did not have the necessary precision. Increasing the back pressure on the mixing system only reduced the gas surging problem. A minimum residence time may be required for adequate mixing of the components.

All samples (except number one) were mixed with a pre-formed foam in a blender. A water based foam of 85 to 90% quality was prepared with surfactant concentrations of 0.3 to 0.4 percent. The cement slurry was then mixed separately and blended with the foam.

All the foam cement samples in this experiment met the A.P.I. water requirement of 0.44 cc/gm (5.0 gal/sack). The water volume used in the creation of the foam was subtracted from the mix water of the dry cement in order to meet this requirement.

The volume of foam was normally constant before and after addition of the cement slurry. This feature allowed ready prediction of the quality up to approximately 75%, at which time a significant reduction in volume accompanied the addition of the cement. Subsequent investigation indicated that the cement slurry (mixed at reduced water ratios) was in competition with the foam for water. Qualities higher than 75% could only be obtained with water concentrations in excess of 0.44 cc/gm.

The way in which additives are used must be carefully considered. The addition of calcium chloride to the cement slurry results in the normal reduction of viscosity and setting time of the foam cement. When calcium chloride is added with the foaming agent, the foam cement is noticeably thicker and produces heat, indicating a flash set of the cement. Other additives were found to give good results when mixed with the foaming agent and poor results when mixed with the cement slurry.

Samples which were tested for permeability, porosity, and pore size were mixed entirely with blenders, then poured into Lucite tubes and sealed. These samples were initially allowed to set for 72 hours, with a subsequent reduction to 48 hours. This difference should not have any significant effect on the measured properties.

The samples tested with 20-40 mesh sandpacks could not be prepared with the sole use of blenders. In these tests, the water base foam was injected into a Lucite tube at 25 psig. The cement slurry was mixed and injected in a like manner. The tube was then placed in a paint shaker and mixed for 30 minutes.

The cement used in all experiments conformed to A.P.I. Class G specifications. The chemical composition and physical properties of this cement are presented in Table 2. The dry cement was sifted through a U.S. Standard 40 Mesh Sieve

(420 micron) prior to mixing.

The surface active agent used in these experiments was Adofoam BF-1. This is a commercially available anionic foaming agent for use with brines or brackish solutions. The surface tension of Adofoam BF-1 in tap water is presented in Figure 1 and Table 1. Measurements were obtained with a DuNuoy tensiometer. The reported surface tensions are average values obtained from repeated tests. Additional tests were conducted with cement filtrate (not reported) and showed little variation from the reported values.

FOAM QUALITY

The bulk volume of the Lucite tubes was measured by subtracting the dry weight of the tube from the weight when full of water. These measurements were accurate to ± 1 cc and were checked by volumetric measurement. Some discrepancy exists between the measured volume and the volume calculated from the tube dimensions. This is because of the lower accuracy in the measurement of the dimensions and irregularities which exist in the tube and end caps.

The weight of the foam cement sample was determined by subtracting the dry weight of the tube from the weight of the tube with the sample. It was then assumed that the cement density was 15.8 lbs./gal. and the density of the gas phase was negligible. The following equation was then used to

predict the fractional quality of the slurry.

$$\text{Quality} = 1 - \frac{(\text{Sample Weight})(8.33)}{(\text{Bulk Volume})(15.8)} \quad (11)$$

The sample was allowed to set and then reweighed. No difference in weight was noted for any of the samples. The plugs were then removed from the ends of the tube and valves were installed. The weight was recorded and the sample was saturated with water (except Sample 13, which was saturated with kerosene). The difference in weight of the sample before and after saturation divided by the bulk volume yields the measured quality. Corrections were made for the lower density of kerosene in Sample 13.

After all tests were conducted, the samples were cut and visually inspected for uniformity. Four of the twenty samples which were prepared contained large void spaces and the data for these samples are not presented. It should be noted that a thin sheath of cement developed against the Lucite in all the samples.

The predicted and measured qualities are shown in Figure 2 and Tables 3 thru 15.

MEASUREMENT OF PERMEABILITY

The apparatus which was used in the determination of permeability is shown in Figure 33. Samples 1 thru 12 were

tested with tap water while Sample 13 was saturated with kerosene. The differential pressure was measured with a mercury manometer which was accurate to 0.025 psi. The flow rates were normally measured over one minute intervals; however, accurate measurements of flow rate in lower quality samples required longer times.

Several notable problems were encountered during flow tests. Very small amounts of air in the sample reduced the water flow rate substantially, in some instances completely blocking flow. The effect of air in the sample was also dependent on the length of time which the sample had been quiescent.

Normal tap water was found to contain sufficient amounts of air to invalidate test results. Water was therefore set in a holding tank and a vacuum placed on the system. The samples were also placed under a vacuum to remove air content.

To ensure complete water saturation, the weight of the sample under atmospheric pressure and 25 psig was measured before and after testing. Samples were tested, allowed to set 24 hours, and tested again. A minimum of three tests was performed on every sample. When all weights were consistent, the flow rates did not vary significantly between tests.

Sample 13 was saturated and tested with kerosene rather

than water. Saturation was obtained with greater ease; however, additional testing could not be conducted with kerosene.

Permeability measurements were also attempted with air. Compressed air was passed through a desiccant (silica gel) and into the sample. Gas flow rates increased initially and stabilized when the sample was dry. Calculated values of permeability were 10 to 20 times higher for gas than for water.

Noticeable shrinkage took place as the sample was dried with air. Cracks developed perpendicular to the direction of flow while the sample diameter was reduced to the point where bonding with the walls of the lucite tube was no longer evident. Shrinkage and cracking were noticeably greater in the higher quality samples. Re-saturating the sample with water returned it to nearly its original volume.

Turbulence was another obstacle in the determination of permeability. All gas flow was turbulent, while many of the samples exhibited a transition from darcian to turbulent flow when tested with water. The transition from darcian to turbulent flow has the same appearance as small gas saturations; i.e., the flow rate is nonlinear with increased pressure differential. The repetition of tests described earlier should adequately discount the

possibility that turbulence was mistaken for gas saturation.

The measured flow rates and pressures are presented in Tables 19 thru 29 and Figures 9 thru 19. Permeability values were calculated from water flow rates in the darcian flow regime and are presented in Tables 3 thru 15 and in Figure 3. These values were checked with the turbulent flow data and the two values were in rough agreement. The gas permeabilities which were calculated are not believed to represent true values and are not presented.

TOTAL AND DISPLACED POROSITY

The total pore volume of the sample was determined from the difference in weight of the dry and saturated sample. The total porosity was then calculated by dividing the total pore volume by the bulk volume of the sample. The values of porosity and pore volume are tabulated in Tables 3 thru 15 and the total porosity versus sample quality is shown in Figure 4.

The "displaced" pore volume was determined from miscible displacement tests which were conducted using fresh water and a dilute solution of NaCl. The volume of the displaced phase which was produced in the effluent was dependent on the flow rate at which the test was run. Within the darcian flow regime, this volume was nearly constant.

Increasing the rate of flow into the transitional or fully turbulent regimes resulted in continued increases of the displaced phase in the effluent. As used in this paper, displaced pore volume is that portion of the sample which conducts flow under darcian conditions.

Values of displaced porosity are tabulated in Tables 3 thru 15 and plotted versus sample quality in Figure 5. The variation in volumes when measured in darcian flow and when measured in turbulent flow are shown in Figure 32 for Sample 2. The volume measured in turbulent flow is in close agreement to the total pore volume as measured by weight, while the displaced pore volume is 39 to 76 percent of the total.

PORE SIZE DISTRIBUTION

The apparatus which was used to determine pore size distribution is shown in Figure 33. The sample was initially saturated with fresh water and displaced by salt solution. The concentration of salt in the effluent was continuously monitored and recorded on a strip chart. Displacement was conducted at differential pressures from 1.5 to 2.5 psi (darcian flow). The total volume of effluent was measured and the test was then run again with fresh water displacing

the salt solution.

The average flow rate was calculated from the measured volume of effluent and the total test interval. Volumes of fresh water and salt solution in the effluent at any point in time were determined from the average flow rate and the conductivity of the effluent. Additional calculations were made as described in the section on theoretical background.

The pore size distribution of the samples are tabulated in Table 31 thru 40 and plotted in Figures 21 thru 30. It should be noted that the distribution is based on the displaced pore volume and not the total pore volume.

FOAM CEMENT WITH UNCONSOLIDATED SAND

Lucite tubes, approximately half full of 20-40 mesh sand, were saturated with water and set in a vertical position. Foam cement was prepared at 25 psig as described earlier and injected into the top of the lucite tube. The downstream pressure on the tube was held at atmospheric, 15 and 25 psig in the three tests which were run.

The cement did not enter the sand whereas the majority of the gas phase did pass into the sand. The volume of gas could not be measured with the equipment available. The volume of water effluent was measured and was less than the original volume of water in the tube.

Injection of foam cement was continued for 30 minutes, at which time compressed air at 25 psig was held on the upstream end of the tube for an additional 24 hours. The rate at which foam cement entered the tube slowed considerably in the first few minutes of the test. Compression of the cement plug (loss of air) continued for approximately two hours.

Once set, attempts to flow back through the tube were not successful. The length of the plug was measured and the sample was removed from the tube. The sample was then dried and weighed. The quality of the plug was calculated with the assumption that the dry density of the cement was 83.3% of the wet density of the cement. This value was obtained from the previous tests in this experiment.

The quality which was calculated is the average value, and it was noted that a gradation from neat cement to a high quality foamed cement existed in the plugs. The plugs of cement could not be removed intact from the tube; so, determination of this quality change could not be made.

The pertinent data from these tests are presented in Table 18.

FILTER LOSS OF FOAM CEMENT

Foam cement was placed in a standard A.P.I. low pressure-low temperature filter press and tested at 50 psig. The

reduction of pressure from 100 psi to 50 psig was necessary to obtain accurate measurements. The quality of the foam cement was determined by weight and was measured at 12 psia, not at 50 psig.

The measured values of water loss are reported in Table 17 and in Figure 8. The foam loss is also presented in Table 17 and it is emphasized that these values do not represent the total loss of the foam cement. The amount of free air lost was not measured.

DISCUSSION OF RESULTS

In this section, the experimental results are discussed. This discussion includes an evaluation of the tests conducted on set samples of foam cement, the tests conducted on foam cement slurries, the effect of experimental procedures on the results, and recommendations for further study.

HARDENED FOAM CEMENT

The relationship between the quality predicted by the slurry weight and the quality measured by saturation of the set cement with water is shown in Figure 2.

It was anticipated that the predicted and measured qualities would be equal; however, the data indicates a small but distinct variation. At high qualities, the foam cement probably has a higher water concentration than 0.44 cc/gm, which would reduce the cement density and produce some error in the predicted quality. This theory is born out by the fact that water ratios higher than 0.44 cc/gm were required to produce foam cement with qualities higher than 75%.

At predicted qualities near 52%, the lower measured quality is because of heterogeneities in the sample. It is

postulated that some of the individual bubbles remain intact and are therefore not saturated with water.

Shrinkage or expansion of the cement as it sets does not appear to be a significant factor. If it were, the measured values of quality would be consistently higher or lower than the predicted values.

The thin sheath of unfoamed cement which developed against the Lucite should not have a material effect on the data obtained in these experiments. This volume is small in comparison to the total sample volume and should effectively increase the quality by a similar amount in all the samples. This effect does not bode well for field applications of foam cement. Raza¹⁷ has noted that oils reduced the foamability of water base solutions, which is the same effect of the oil-wet Lucite in these experiments.

The total porosity of foam cement is consistently higher than the quality (Figure 4). There appears to be a discrepancy between these results and those reported by Aldrich, who found that the porosity and quality were equal. The difference in results is because Aldrich used the pore volume and bulk volume of the dry foam cement to calculate porosity, while the pore volume and bulk volume of the wet cement was used in this study.

The total pore volume was obtained in this study from the difference in weight of the dry and saturated samples.

In samples with high permeabilities, similar values were obtained during miscible displacement tests at highly turbulent flow rates. The fact that these two methods yield similar results is significant for several reasons.

The free water is collected primarily on the cement surface and very little water is contained in the matrix. The shrinkage of the foam cement as it is dried is caused by pore volume shrinkage rather than the cement matrix. This, in turn, explains why the higher quality samples exhibit greater shrinkage when dried.

Drying of foam cement is analogous to the squeezing of a sponge. The reduction in bulk volume is equal to the reduction in pore volume, which results in a lower porosity. This is the reason why the results of this study and those obtained by Aldrich do not agree.

Turbulent displacement tests indicate that the total pore volume is interconnected. A "displaced" porosity is defined in this study as that portion of the bulk volume which conducts flow in the darcian flow regime. In foam cement, the displaced porosity was found to be lower than the total porosity and lower than the measured quality (Figure 5). Two possible reasons for this difference are dead end pores and capillary pressure.

If the film of a gas bubble is broken in only one place, the bubble volume would contribute to the total pore volume

but not to the flow path. Eddies in the turbulent flow regime may displace this volume while the streamlined darcian flow would not displace it.

Capillary pressure is a factor because of the desorption of surfactant from the cement surface. The entrance of displacing fluid into a bubble would require a differential pressure in excess of the capillary pressure. The capillary pressure of the smaller pores may not be exceeded by the low differential pressures in the darcian flow regime.

Displacement tests were not conducted in a manner which would distinguish between dead end pores and the effects of capillary pressure. The calculation of pore size (equation 9) is not affected by the pore volume. The distribution of pore size in this paper is based on the displaced pore volume rather than total pore volume.

The pore size distribution of the foam cement samples (Figure 21 thru 30) is much wider than that of a graded sand (Figure 31). A least squares fit of the minimum, maximum, and median pore size versus quality is shown in Figure 7. This fit of data indicates that the pore size approaches zero at a measured quality of 46 to 49%. This is reasonably close to the theoretical onset of permeability at a predicted quality of 52%.

The increase in pore size with measured quality explains the rapid increase of permeability (Figure 3). The permeability and pore size of a 75% quality foam cement is comparable to a

20-40 mesh sandpack with a permeability of 28 darcies and a median pore size of 20 microns. Klinkenberg found a one darcy sandstone had a median pore radius of 6 microns, which compares favorably to a foam cement quality of 60%.

FOAM CEMENT SLURRIES

The primary point of interest in this study is the fact that foam cement will not enter a 20-40 mesh sand. Additional tests (not reported) with unfoamed cement slurries would also not enter a 20-40 mesh sand. The use of foam cement for sand consolidation appears to be limited to larger sands.

The loss of the gas phase from the foam cement is significant to any application. Considering the high fluid loss of neat cement, the loss of the gas phase in foamed cement is not a surprising development. Additives to control water loss were tested. These tests were not encouraging; however, they were extremely limited in scope. King has reported reduction in fluid loss for water base foams with the use of agents which "toughen the bubble skin". These are proprietary items and could not be tested in this study.

Filter loss tests were undertaken to determine the effect of quality on the water loss of the slurry. It can be seen from Figure 8 that the initial spurt loss decreased with increasing quality. This is in contrast to the incremental

water loss from 30 to 60 seconds, which is virtually constant over the quality range. Extrapolation of the water loss to 30 minutes as prescribed by A.P.I. test procedures would give virtually the same water loss over the entire range of qualities.

EFFECT OF EXPERIMENTAL PROCEDURE

The manner in which foam cement is prepared has a major effect on the properties of the finished product. The results obtained in this study will not be representative of foam cement prepared in a different manner. All samples, except Sample 1, were mixed with the same procedure and should give comparable results. The properties of Sample 1 were noticeably different from the other samples.

Permeability measurements were conducted with water, and other fluids may be expected to give different results. The single test of Sample 13 indicates that this difference may not be significant.

Several factors in the measurement of pore size distribution and displaced porosity should be noted. The diffusion coefficient of NaCl and Adofoam BF-1 will have an effect on the results which were obtained. High permeability samples were tested in a matter of minutes while the low permeability samples required several days of testing. In addition, the desorption of surfactant would vary with the quiescent period

prior to testing.

Filter press data were obtained with an upstream pressure of 50 psig rather than the standard A.P.I. pressure of 100 psig. This reduction was required to obtain any degree of accuracy in measurements. An additional factor in these tests was the preparation of the foam cement at 12 psia. Subjecting the sample to 50 psig results in compression of the gas phase, thereby reducing the quality of the foam cement. The change in gas volume is a five-fold decrease and will obviously affect the results which were obtained. Had the sample been prepared at 50 psig, the reverse problem would have occurred; i.e., the volume of gas at 12 psia would be five times the volume at 50 psig.

RECOMMENDATIONS FOR FURTHER STUDY

This study was not successful in demonstrating that foam cement could be applied to sand consolidation. This does not imply that a foamed material cannot be applied to the consolidation of sand. Epoxy, for example, has been used in sand consolidation with some success and it has also been foamed for other applications. Investigation of an epoxy or other plastic resin may be worthwhile.

Foam cement may find application to control of sand production (opposed to sand consolidation) if fluid loss

problems are solved. Further study of foam cement should include the following topics:

1. A detailed study of the surface chemistry of foam cement. Specific points in this study might include the selection of surfactant, optimum bubble size, stability, effects of oil contamination, etc.
2. Fluid loss (water and gas) properties of foam cement at different absolute and differential pressures. The effect of bubble size and additives should also be included in this study.
3. Effect of pressure and temperature on the properties of foam cement.

CONCLUSIONS

The following conclusions are reasonably supported in this study:

1. Foam cement, as prepared in this study, cannot be applied to consolidation of 20-40 mesh sand.
2. Under atmospheric conditions, high permeabilities develop in foam cement above a predicted quality of 52%.
3. The total porosity of set foam cement is higher than the predicted and measured quality.
4. Free water collects on the cement surface, rather than the interior of the cement matrix.
5. The foam structure requires a minimum water concentration over and above the minimum requirement of the cement.
6. The water spurt loss of foam cement is reduced with increased quality, but continued water loss is independent of foam cement quality.

FIGURE 1

SURFACE TENSION OF ADOFOAM BF-1 IN TAP WATER

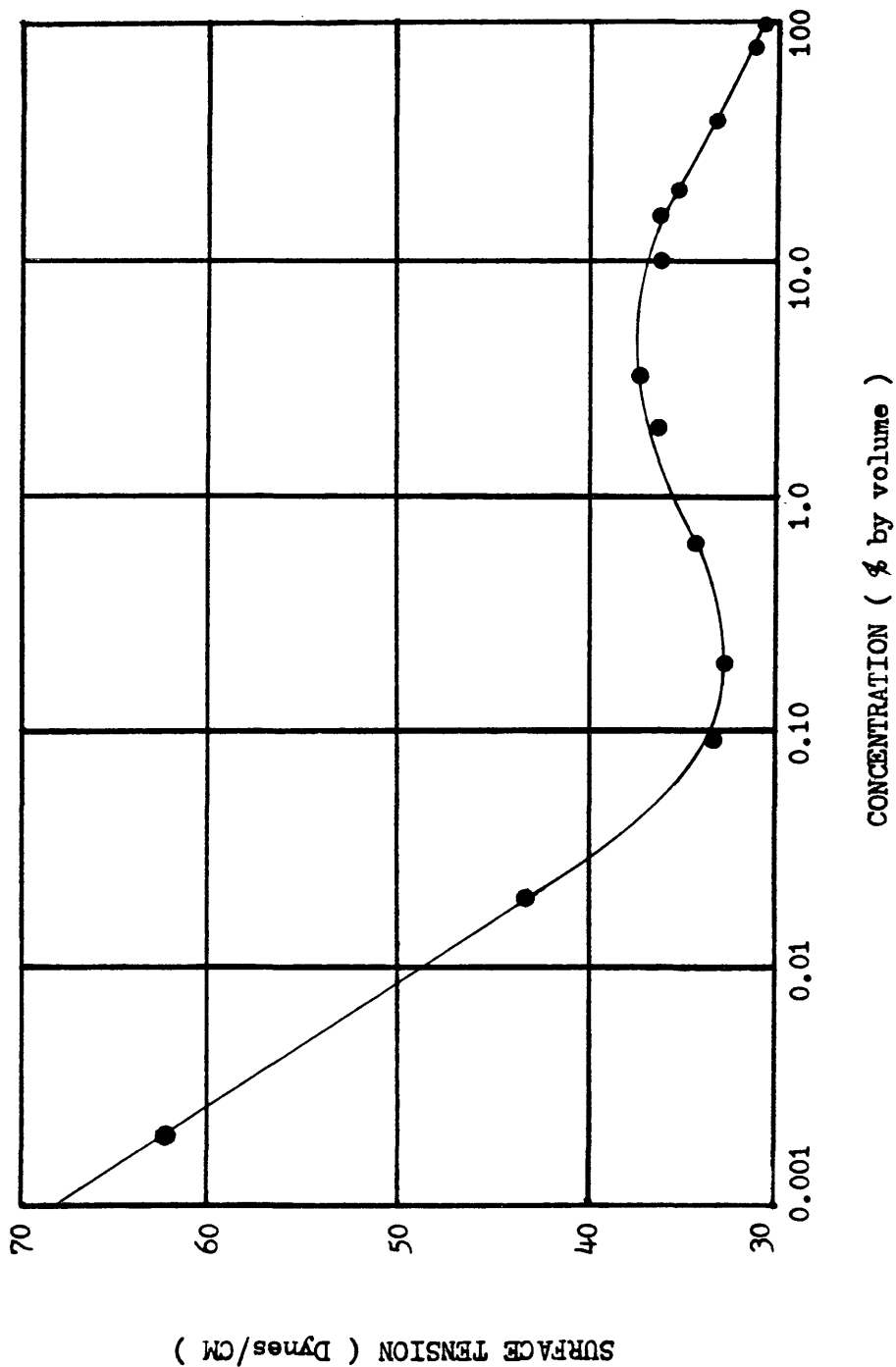


FIGURE 2

PREDICTED AND MEASURED QUALITIES

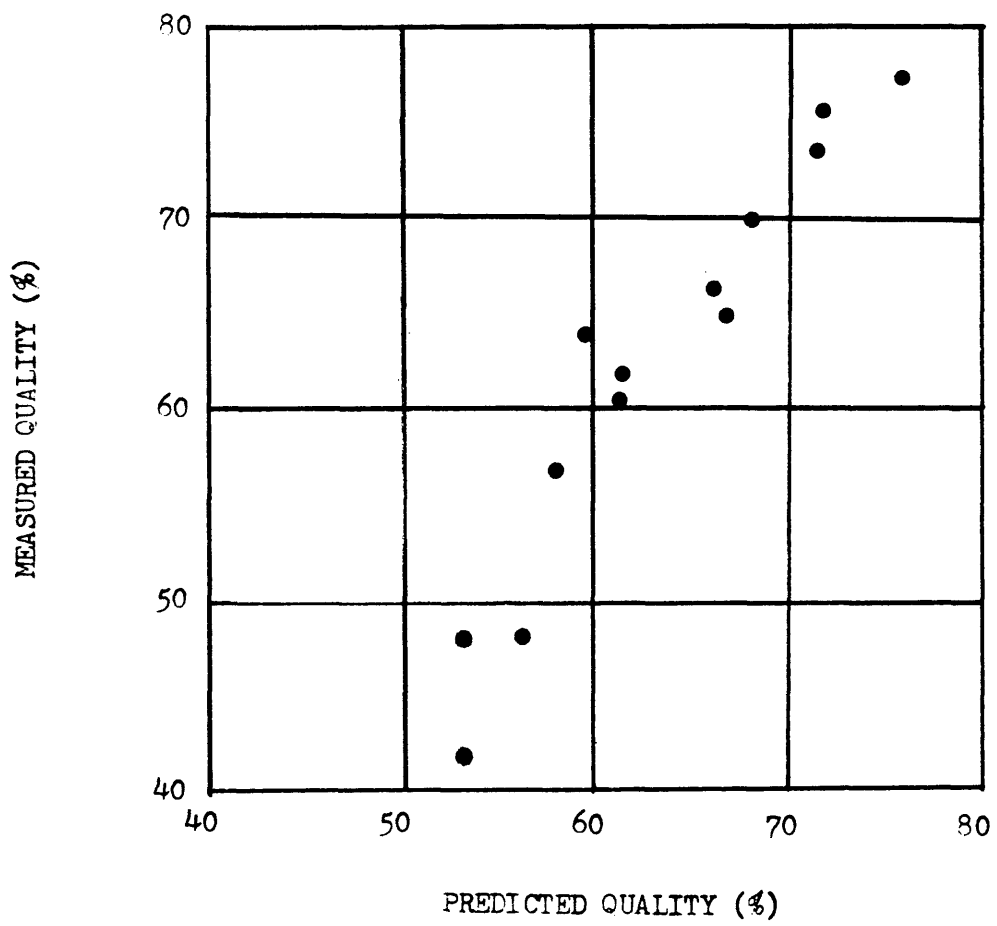


FIGURE 3

PERMEABILITY OF FOAM CEMENT

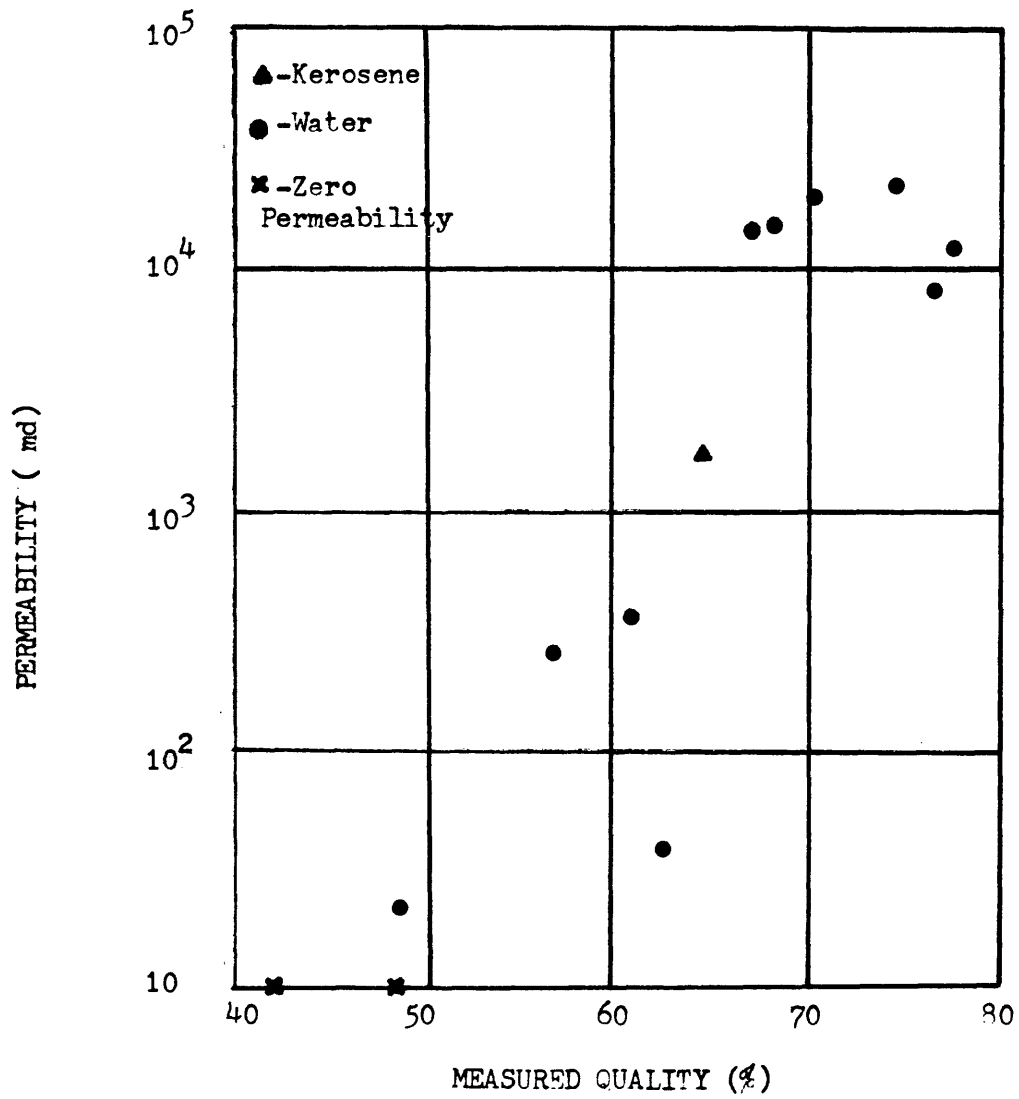


FIGURE 4

TOTAL POROSITY OF FOAM CEMENT

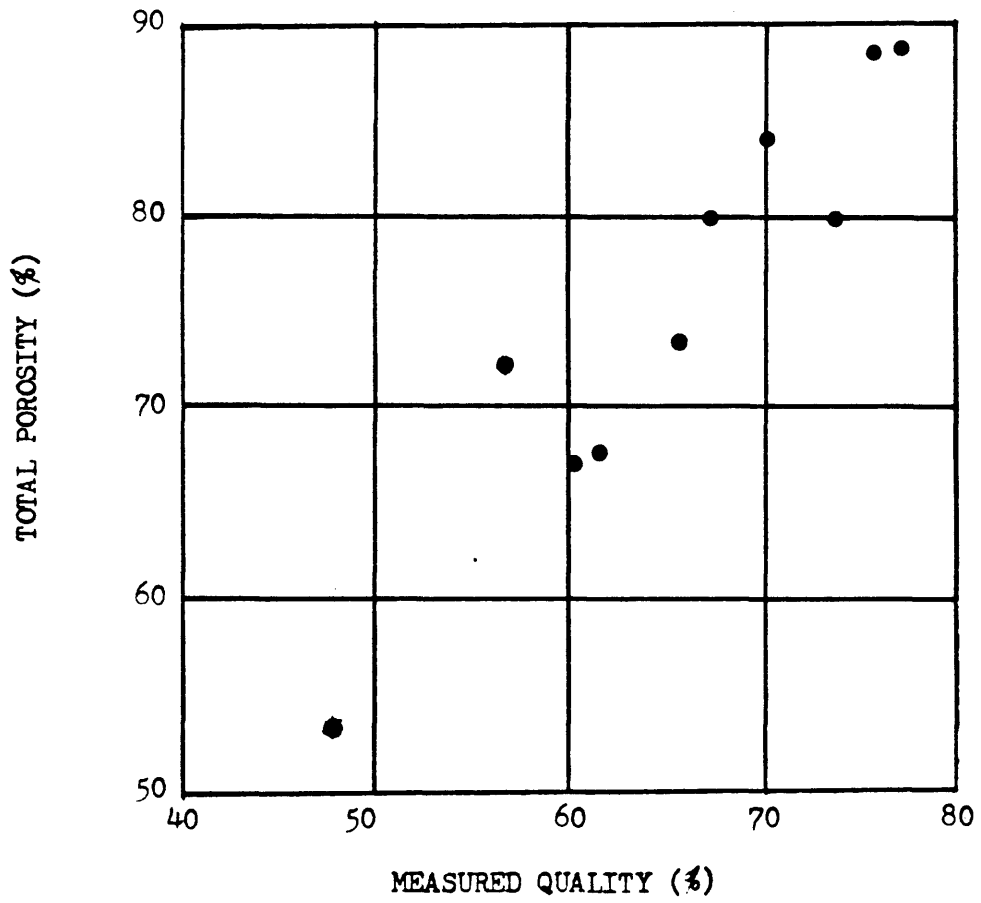


FIGURE 5

DISPLACED POROSITY OF FOAM CEMENT

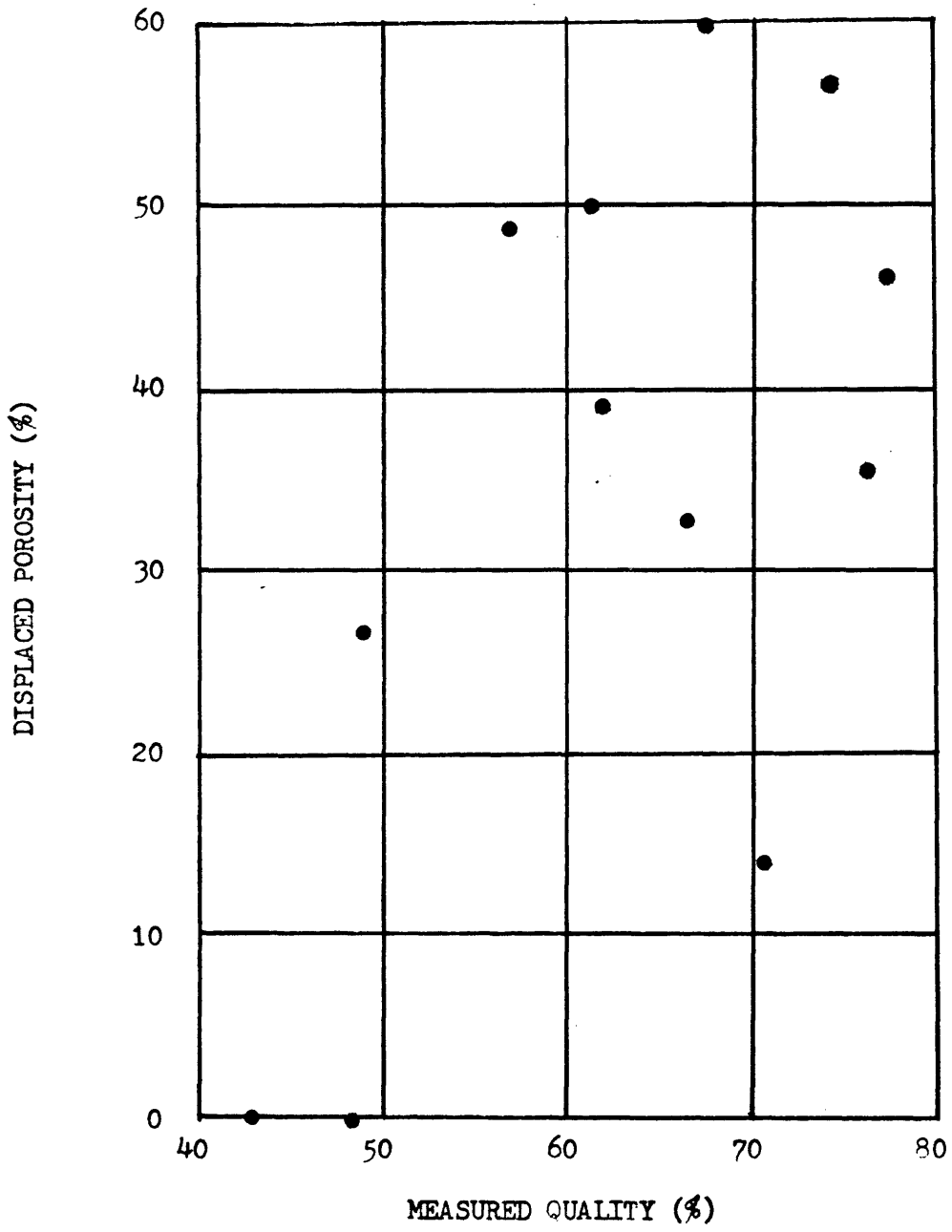


FIGURE 6

INITIAL WATER SATURATION OF FOAM CEMENT

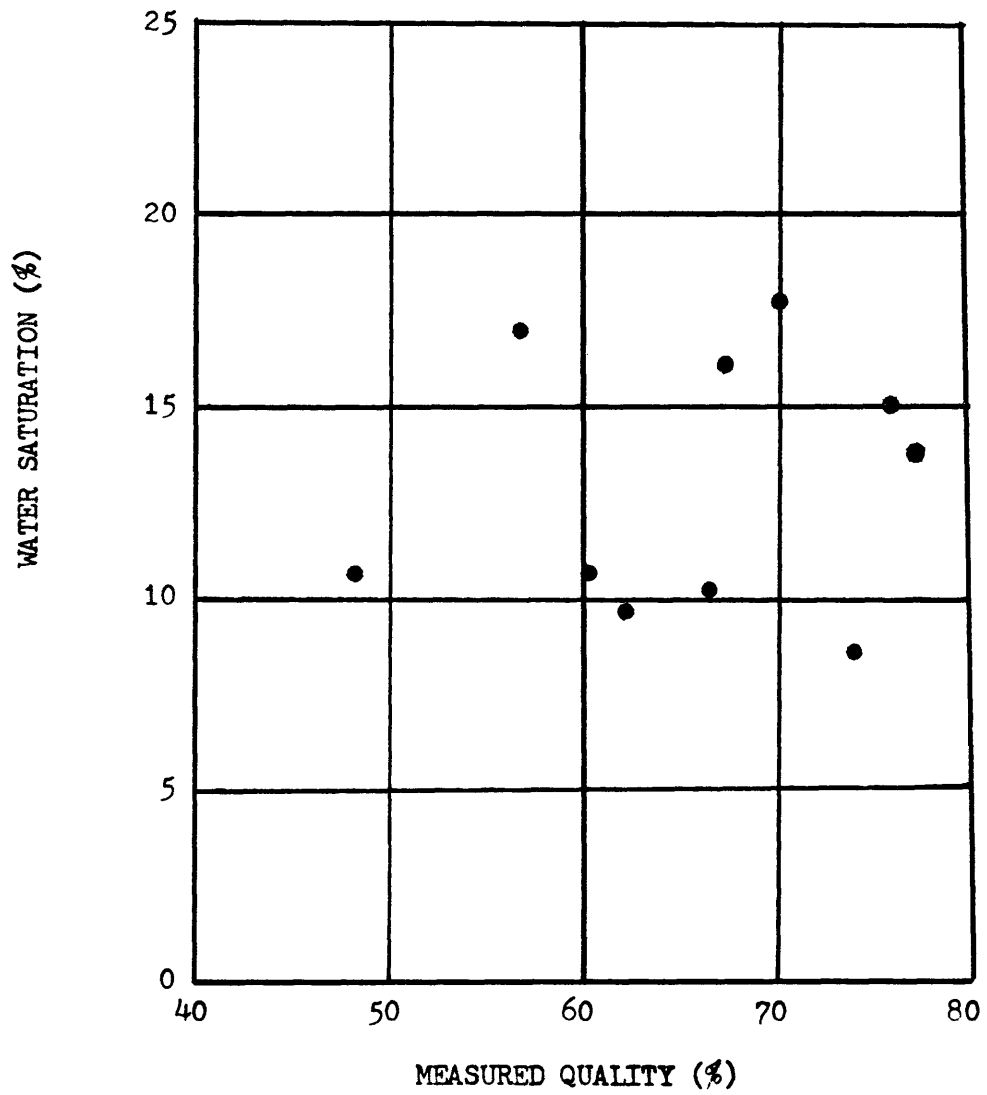


FIGURE 7

MEDIAN PORE SIZE OF FOAM CEMENT

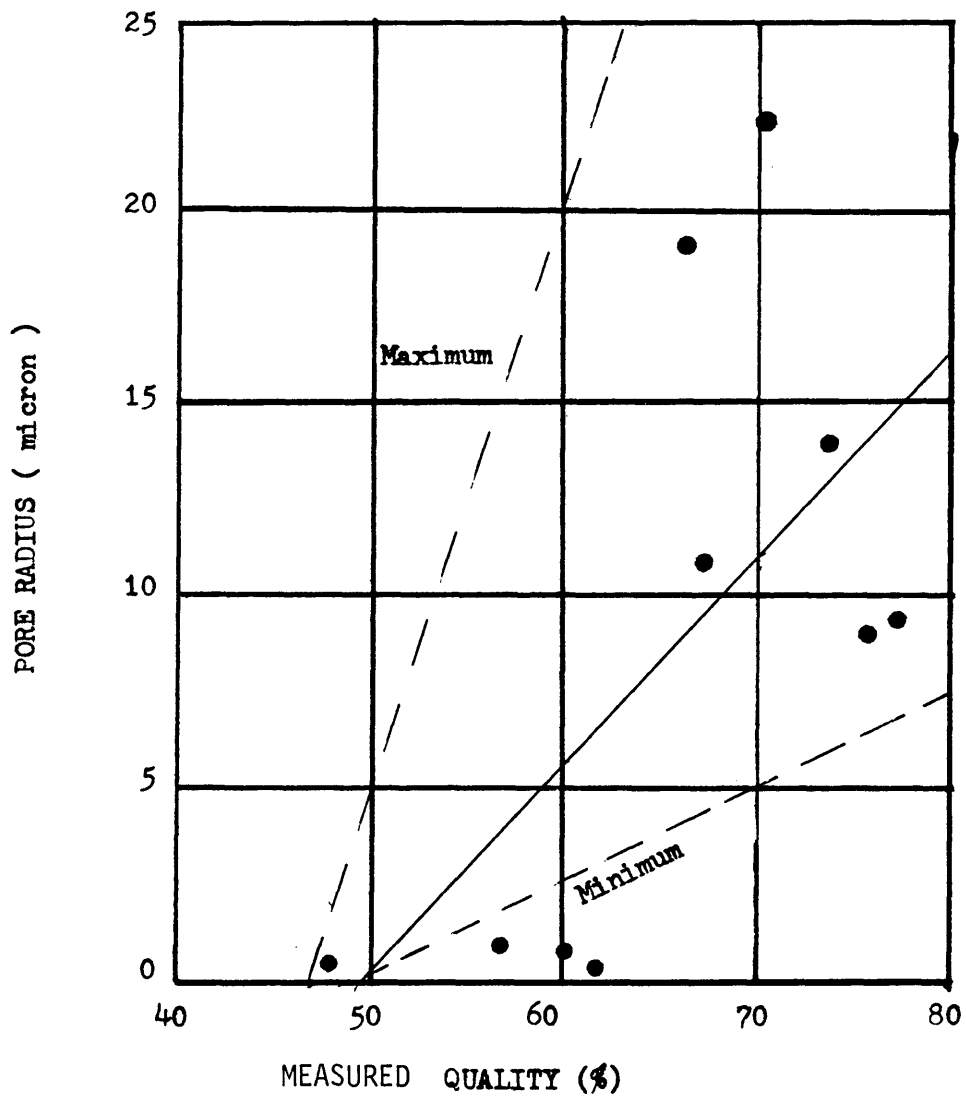


FIGURE 8

WATER LOSS OF FOAM CEMENT

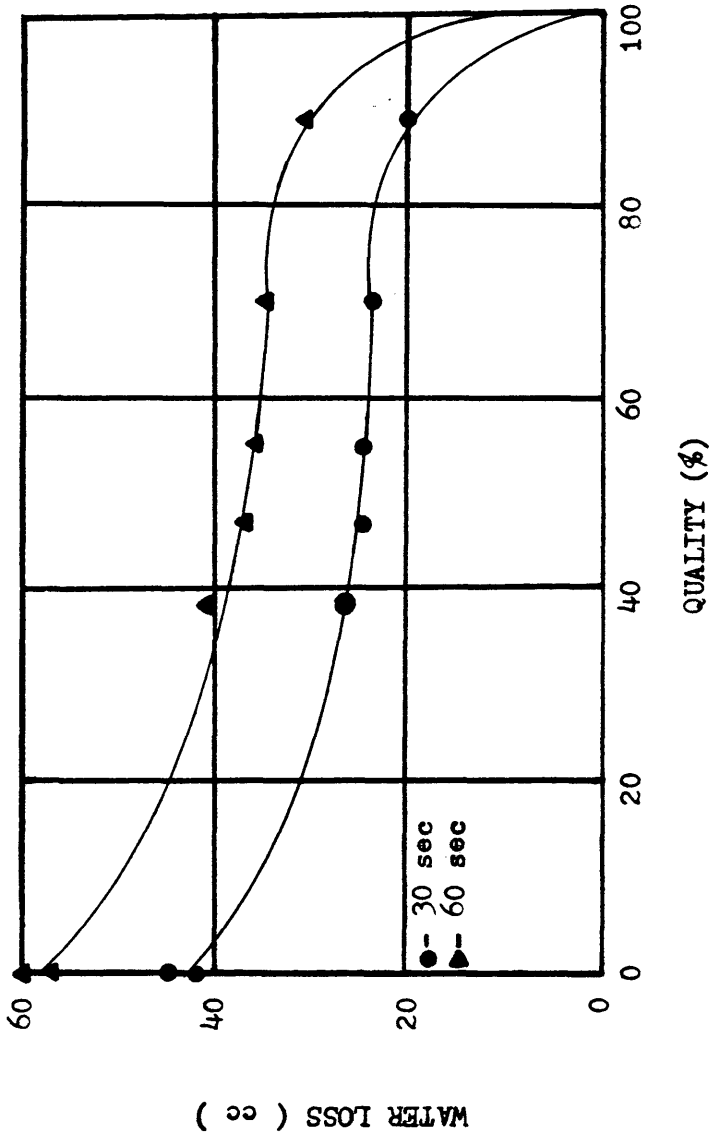


FIGURE 9
DIFFERENTIAL PRESSURE
VERSUS WATER FLOW RATE
SAMPLE 1

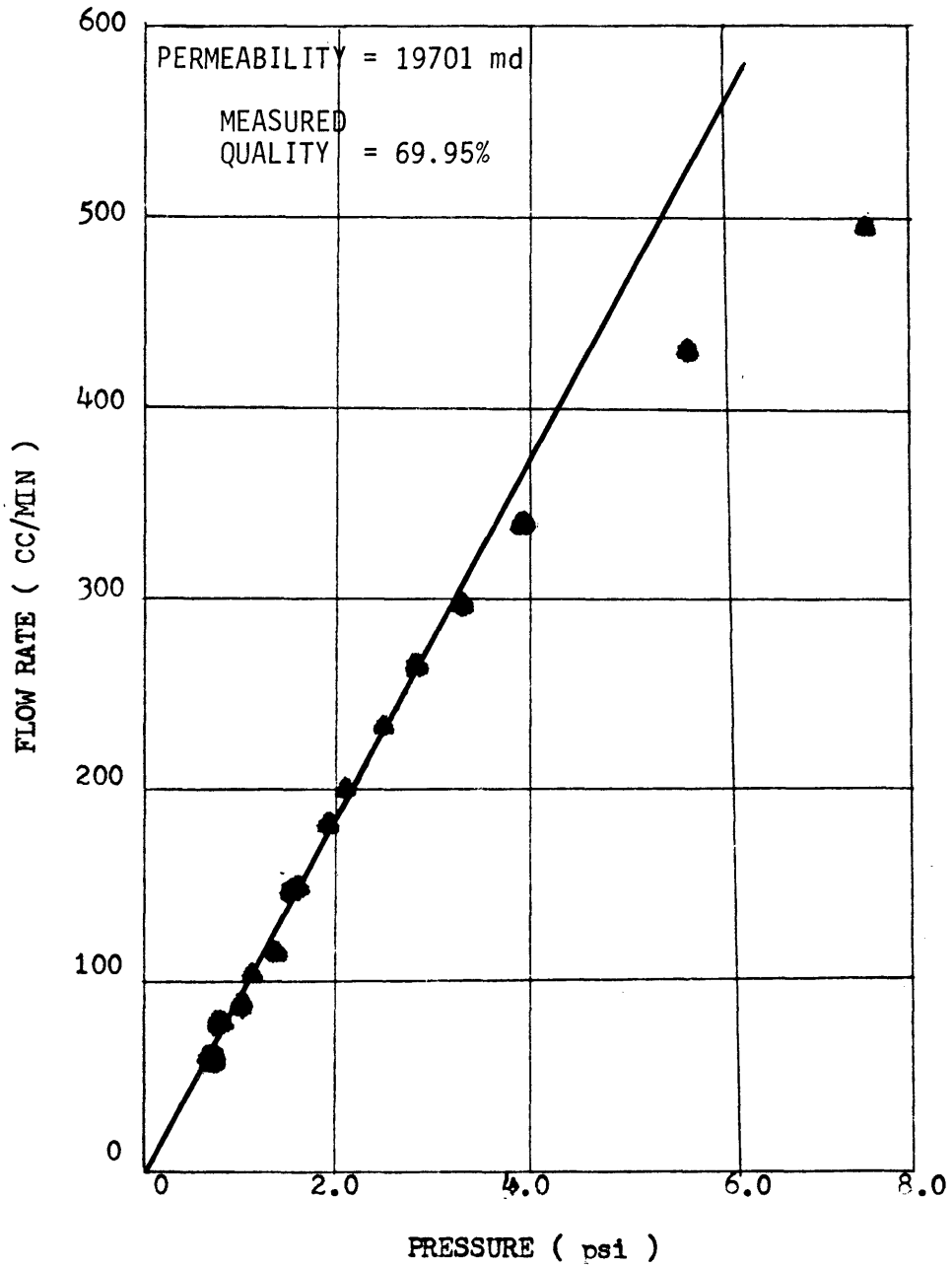


FIGURE 10
DIFFERENTIAL PRESSURE
VERSUS WATER FLOW RATE
SAMPLE 2

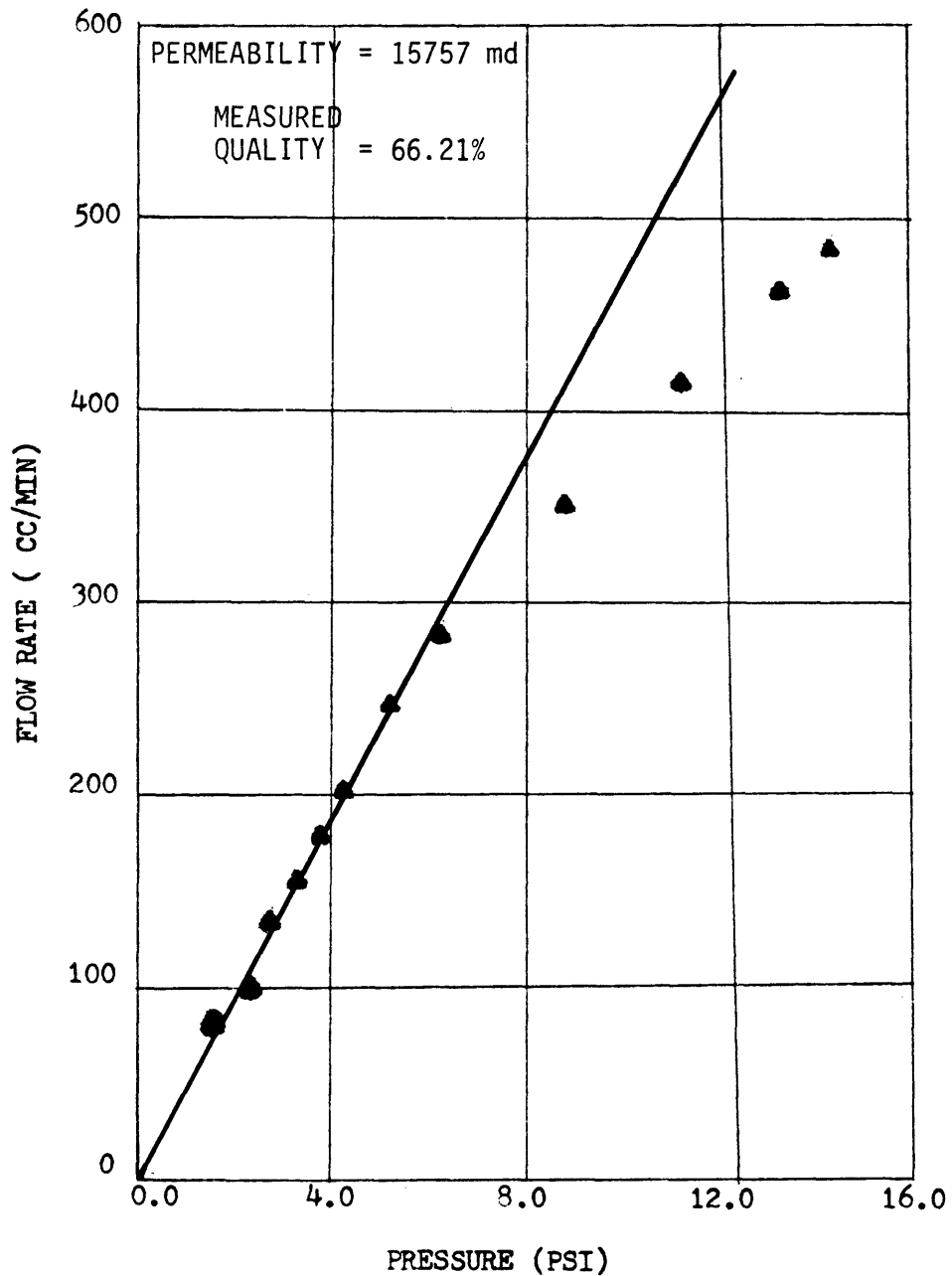


FIGURE 11
DIFFERENTIAL PRESSURE
VERSUS WATER FLOW RATE
SAMPLE 3

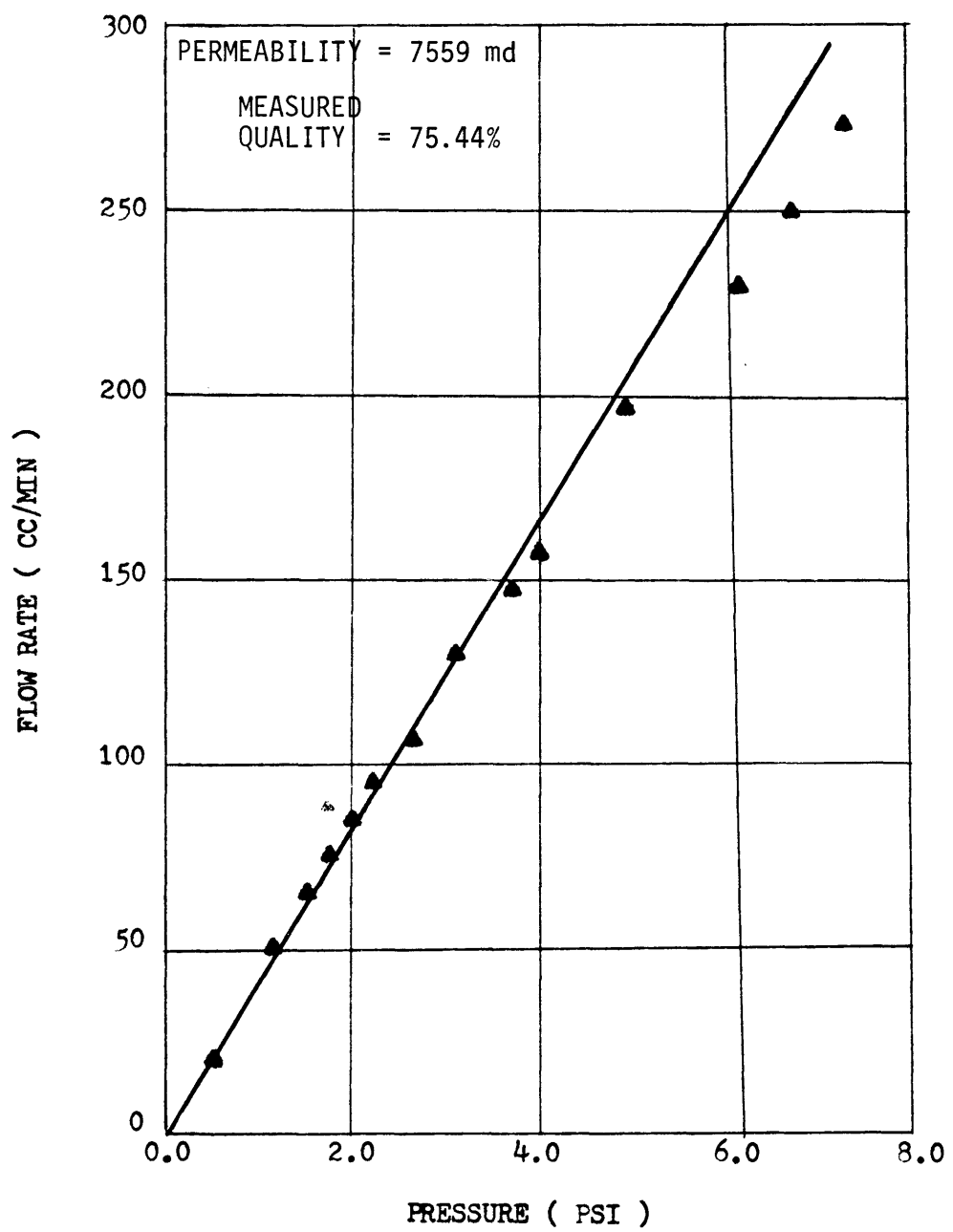


FIGURE 12
DIFFERENTIAL PRESSURE
VERSUS WATER FLOW RATE
SAMPLE 4

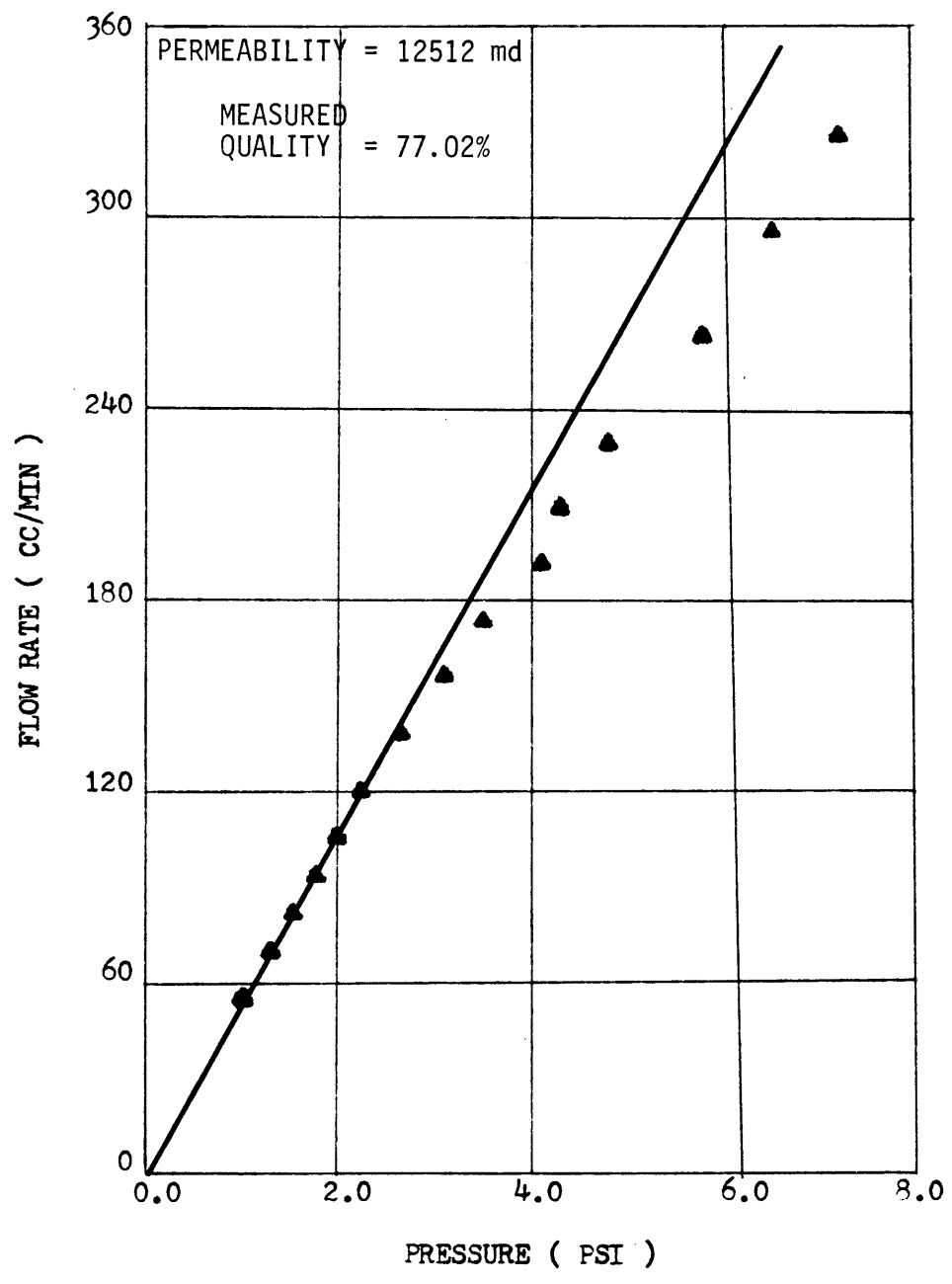


FIGURE 13
DIFFERENTIAL PRESSURE
VERSUS WATER FLOW RATE
SAMPLE 5

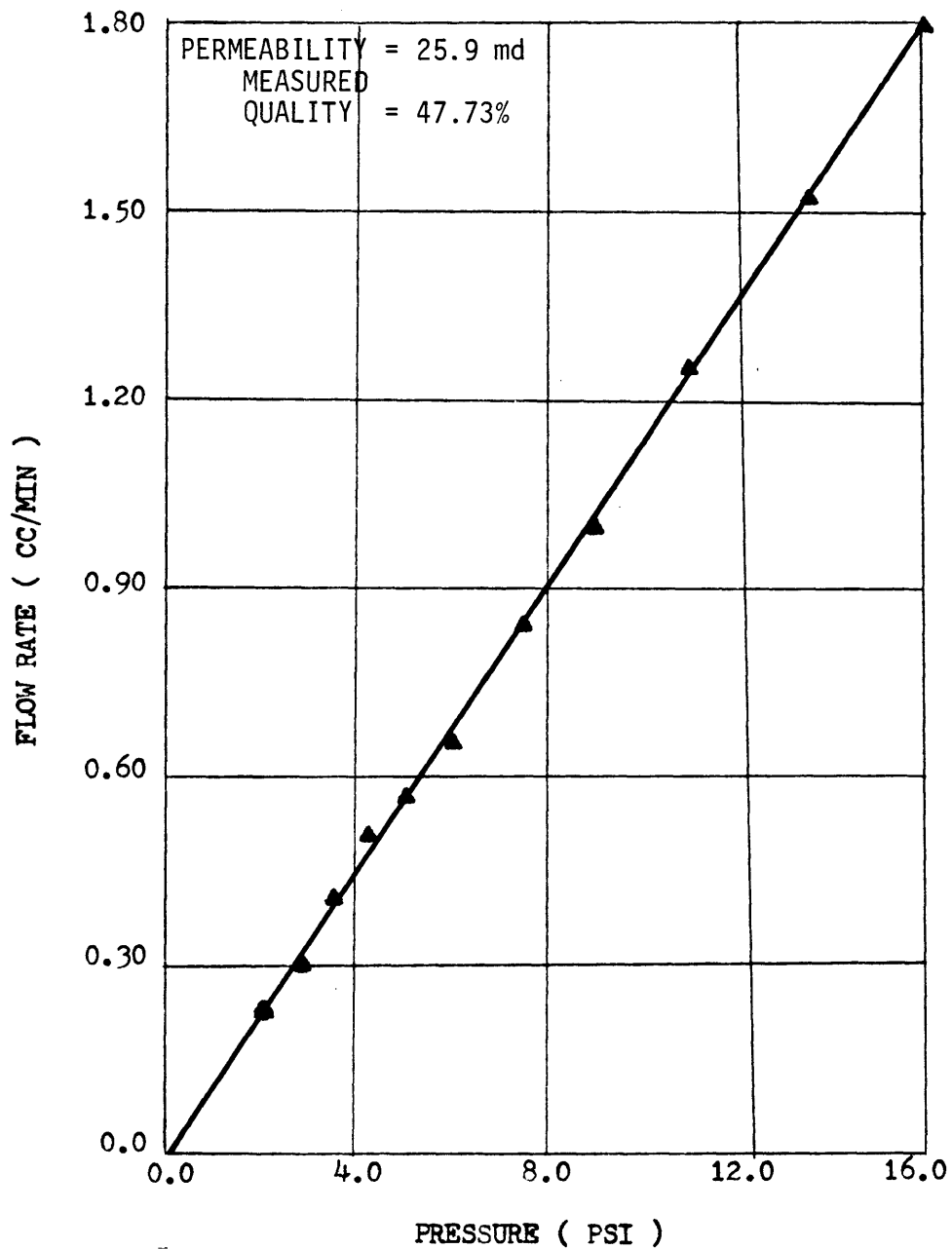


FIGURE 14
DIFFERENTIAL PRESSURE
VERSUS WATER FLOW RATE
SAMPLE 6

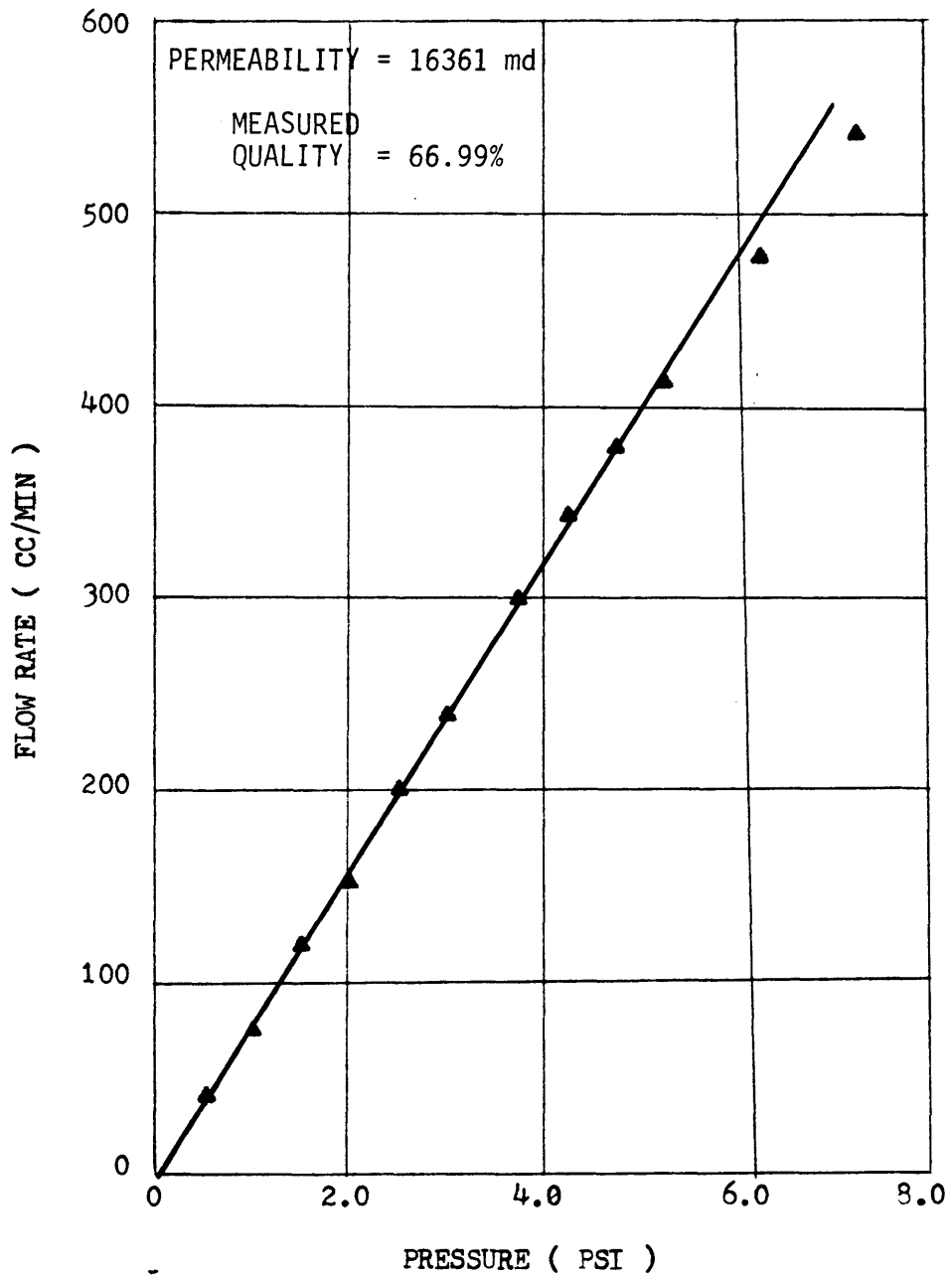


FIGURE 15
DIFFERENTIAL PRESSURE
VERSUS WATER FLOW RATE
SAMPLE 7

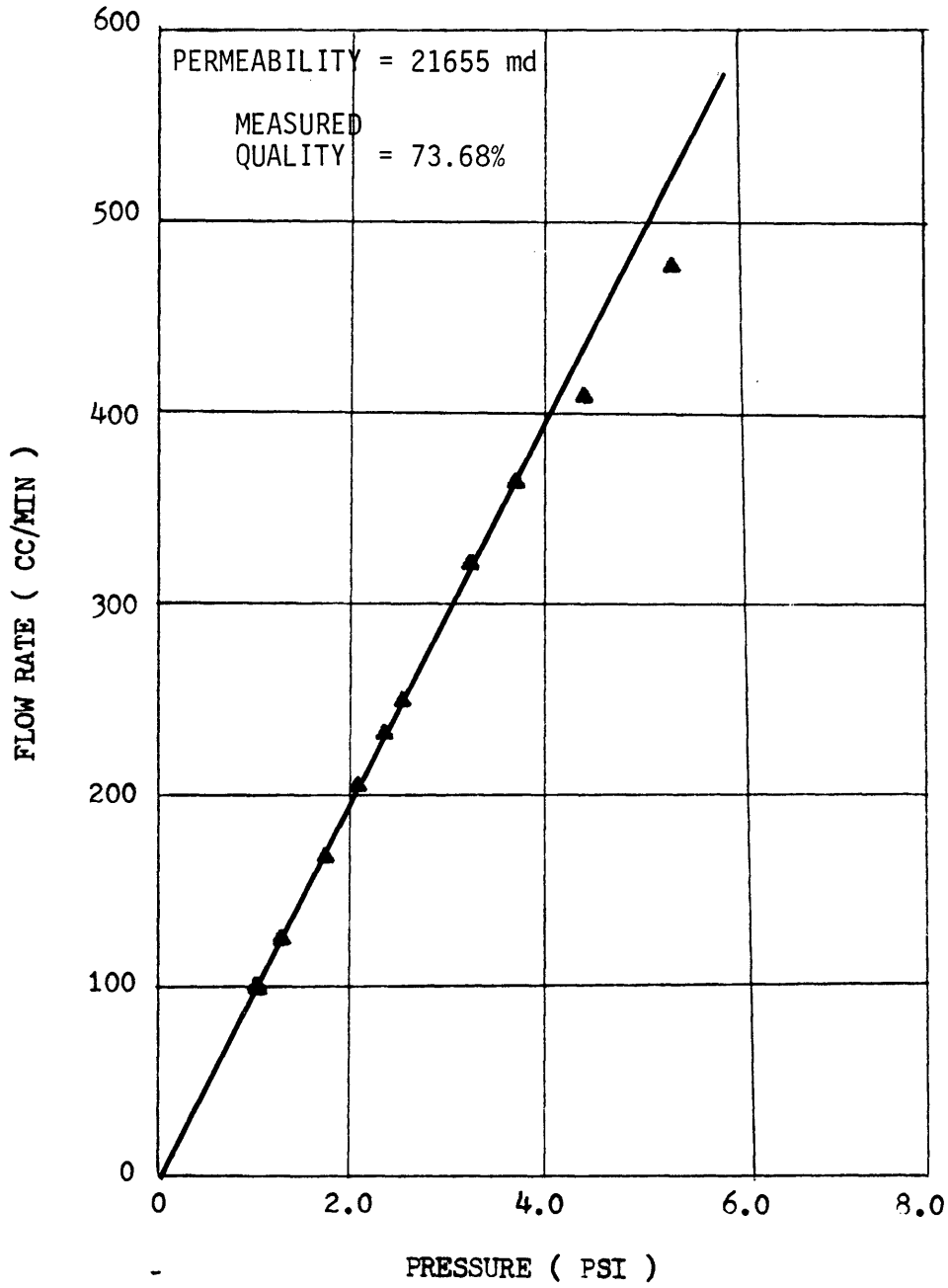


FIGURE 16
DIFFERENTIAL PRESSURE
VERSUS WATER FLOW RATE
SAMPLE 8

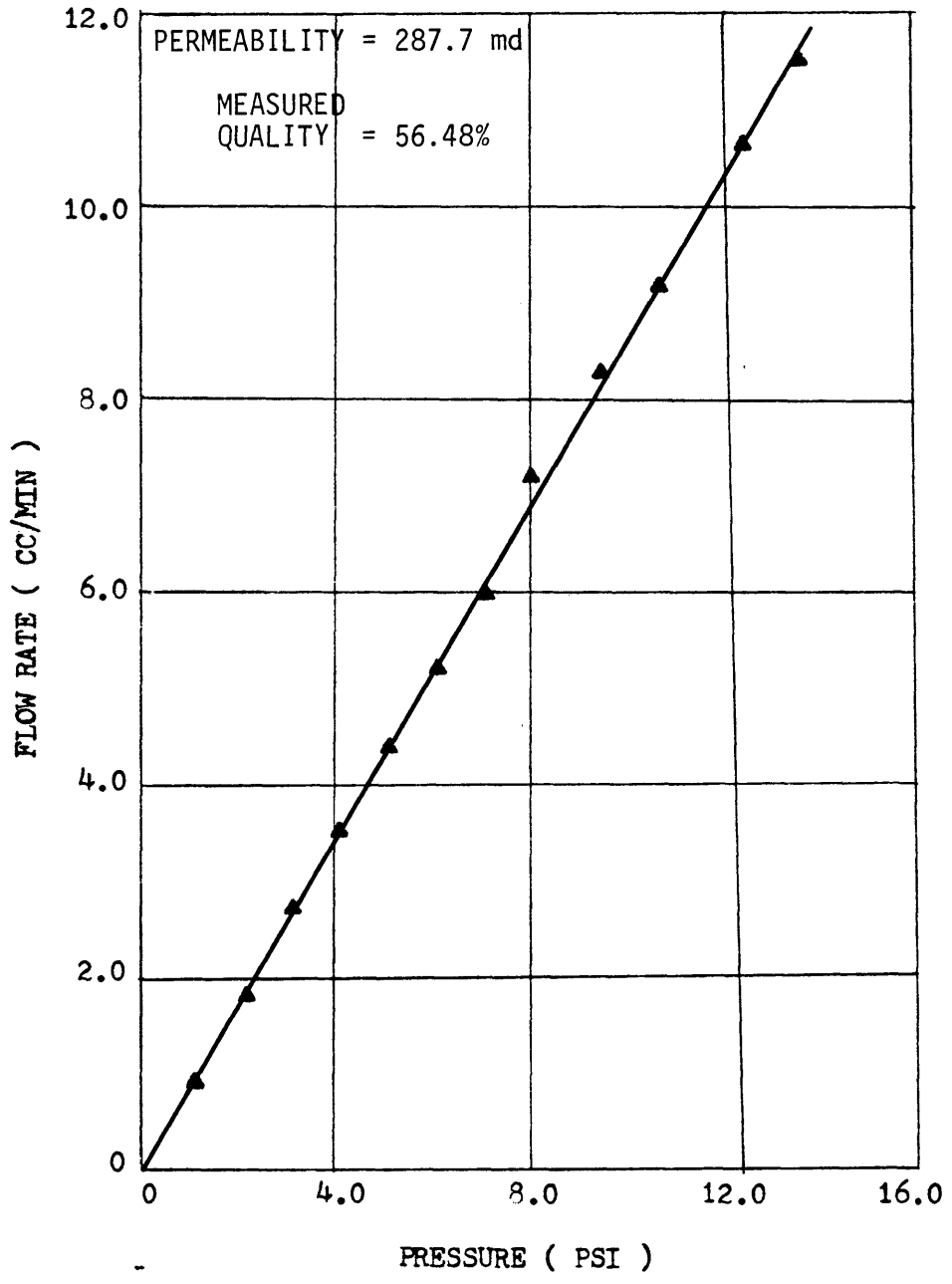


FIGURE 17
DIFFERENTIAL PRESSURE
VERSUS WATER FLOW RATE
SAMPLE 9

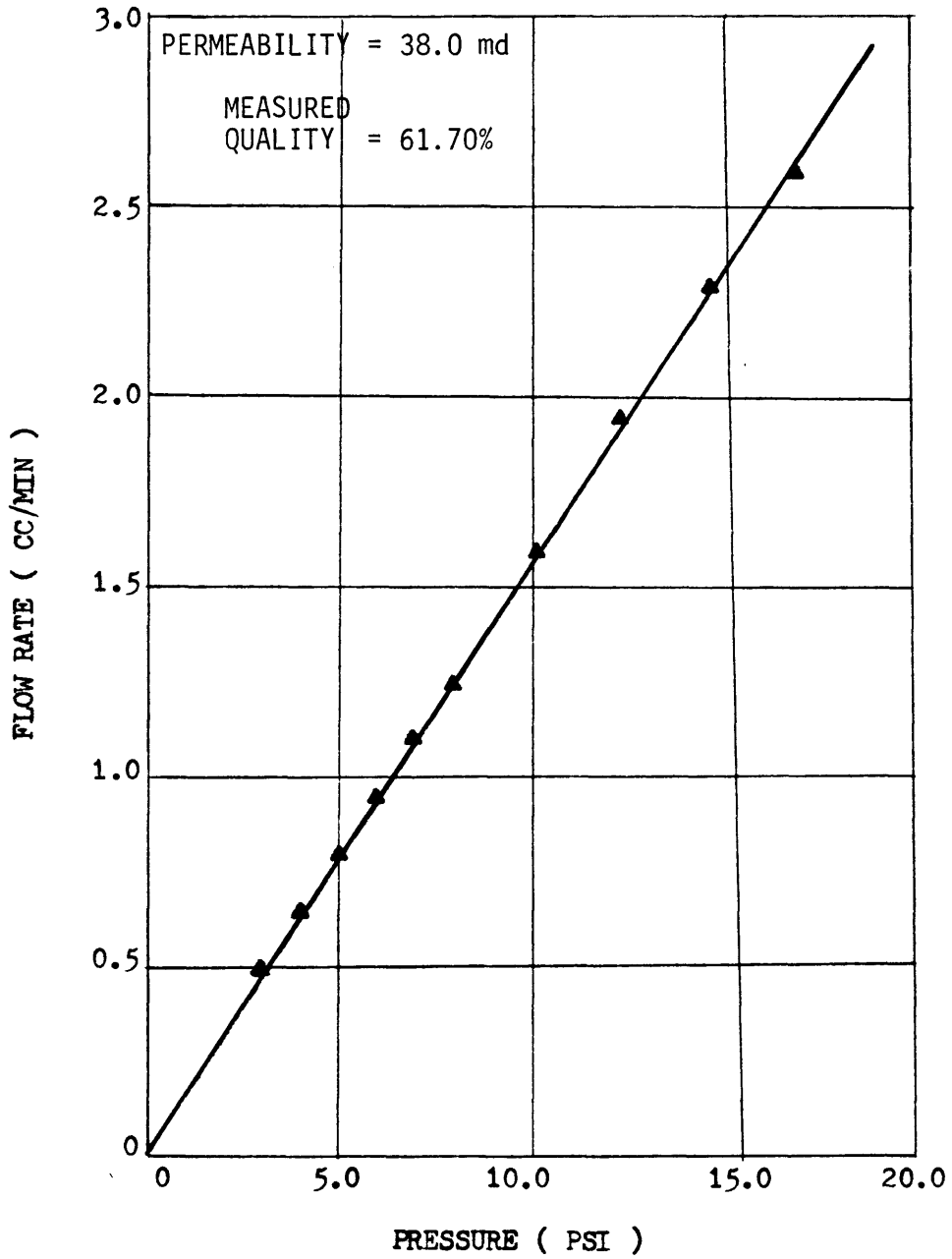


FIGURE 18
DIFFERENTIAL PRESSURE
VERSUS WATER FLOW RATE
SAMPLE 10

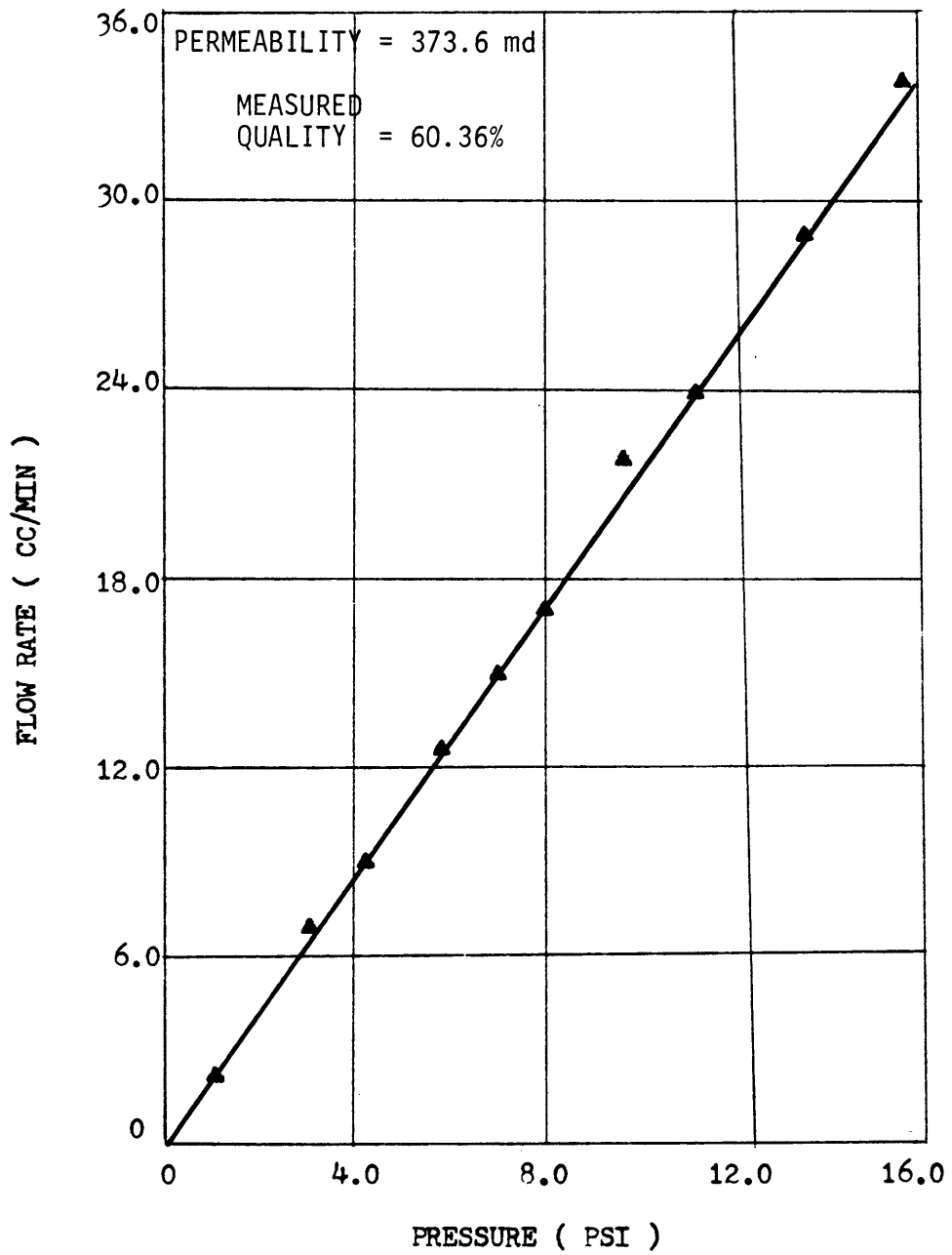


FIGURE 19
DIFFERENTIAL PRESSURE
VERSUS KEROSENE FLOW RATE
SAMPLE 13

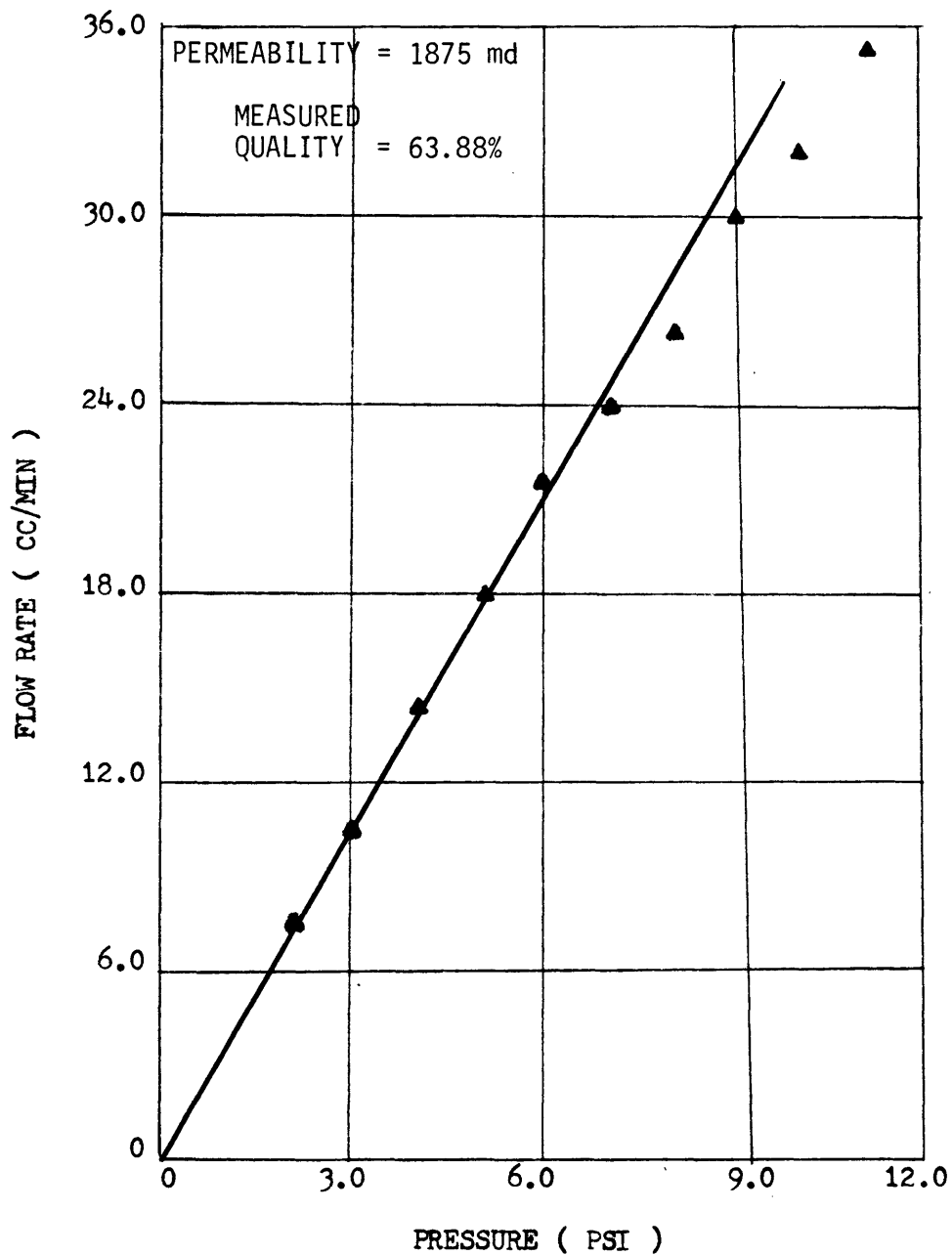
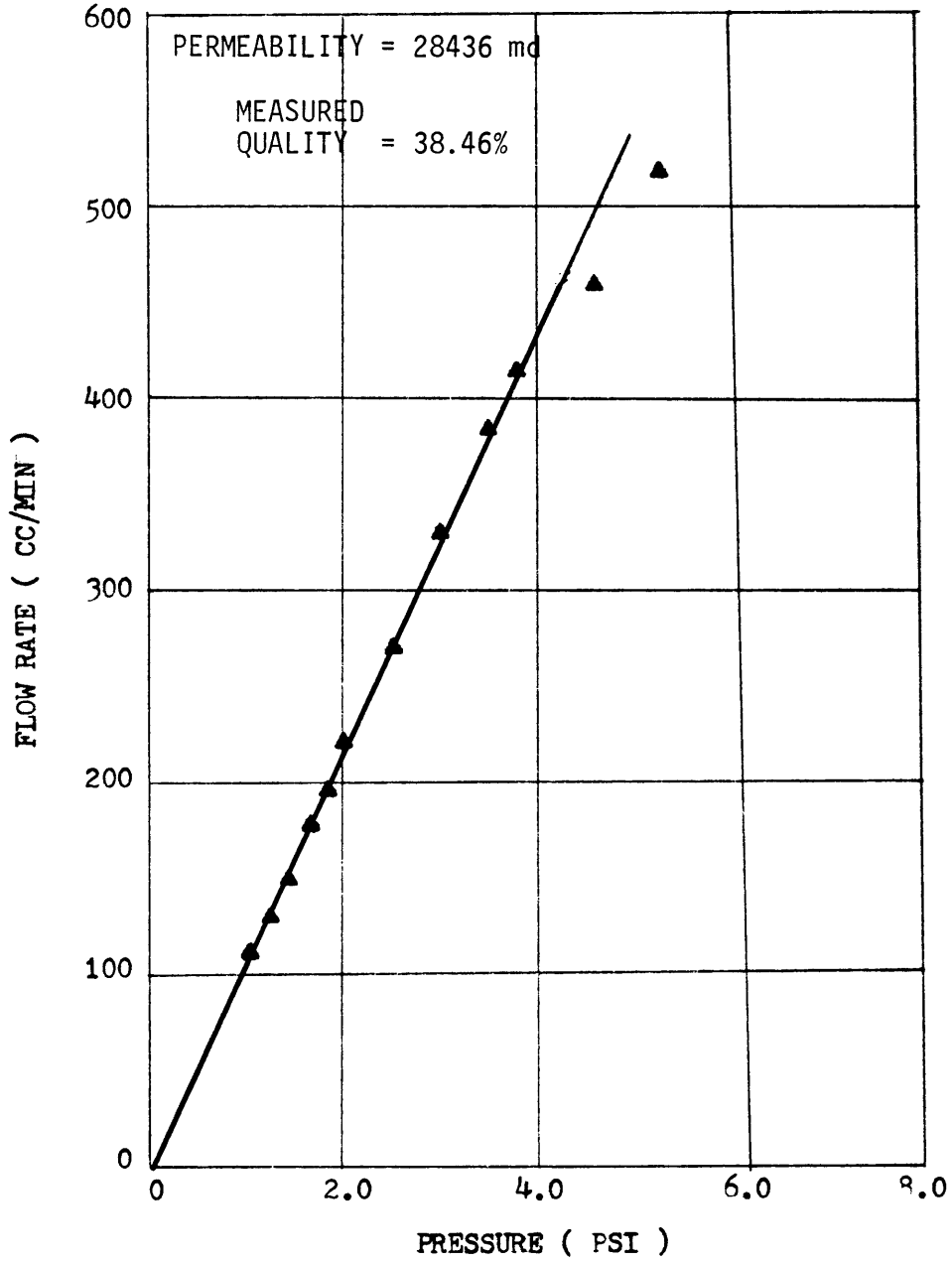


FIGURE 20
DIFFERENTIAL PRESSURE
VERSUS WATER FLOW RATE
20 - 40 MESH SAND



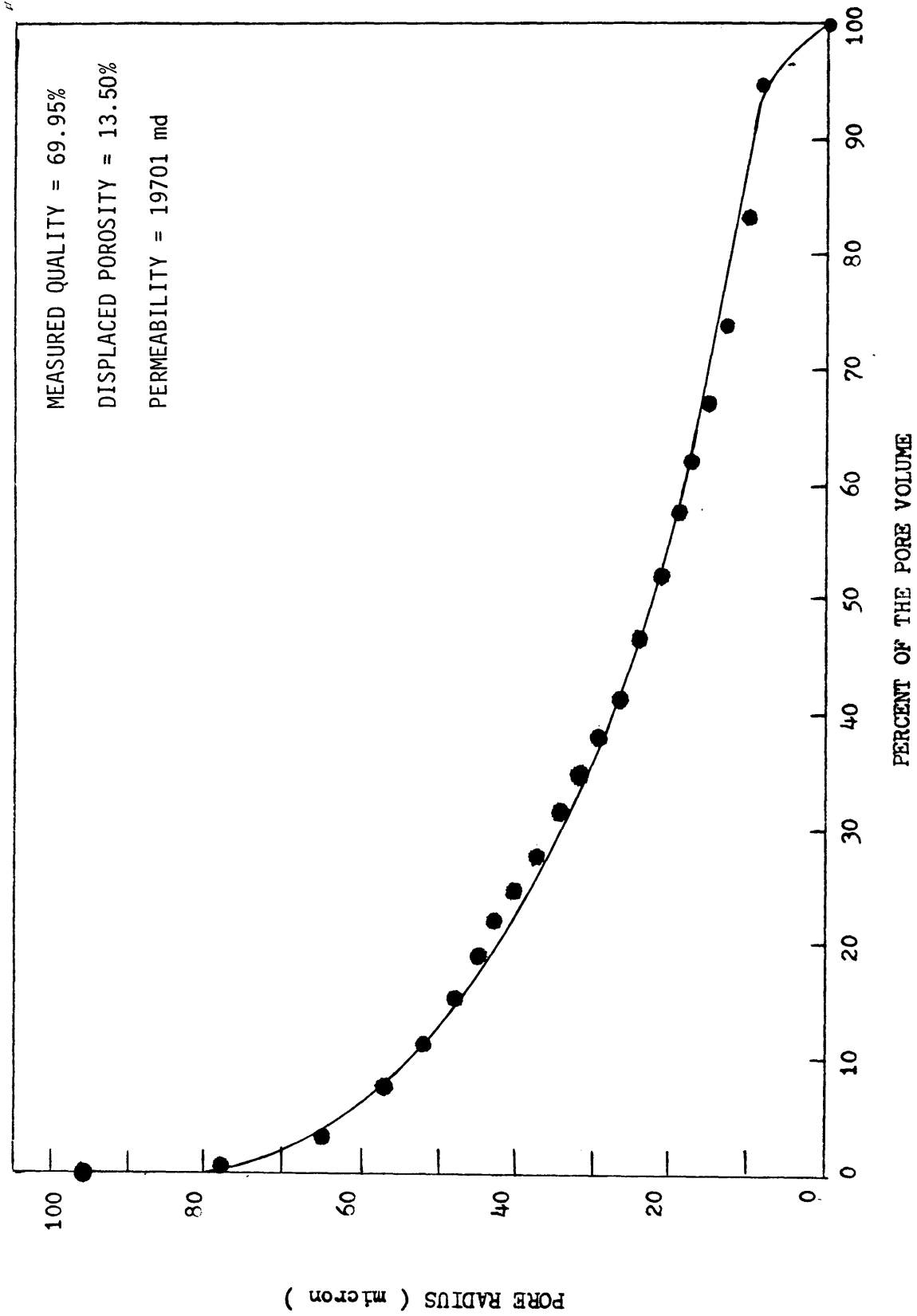


Figure 21: PORE SIZE DISTRIBUTION SAMPLE 1

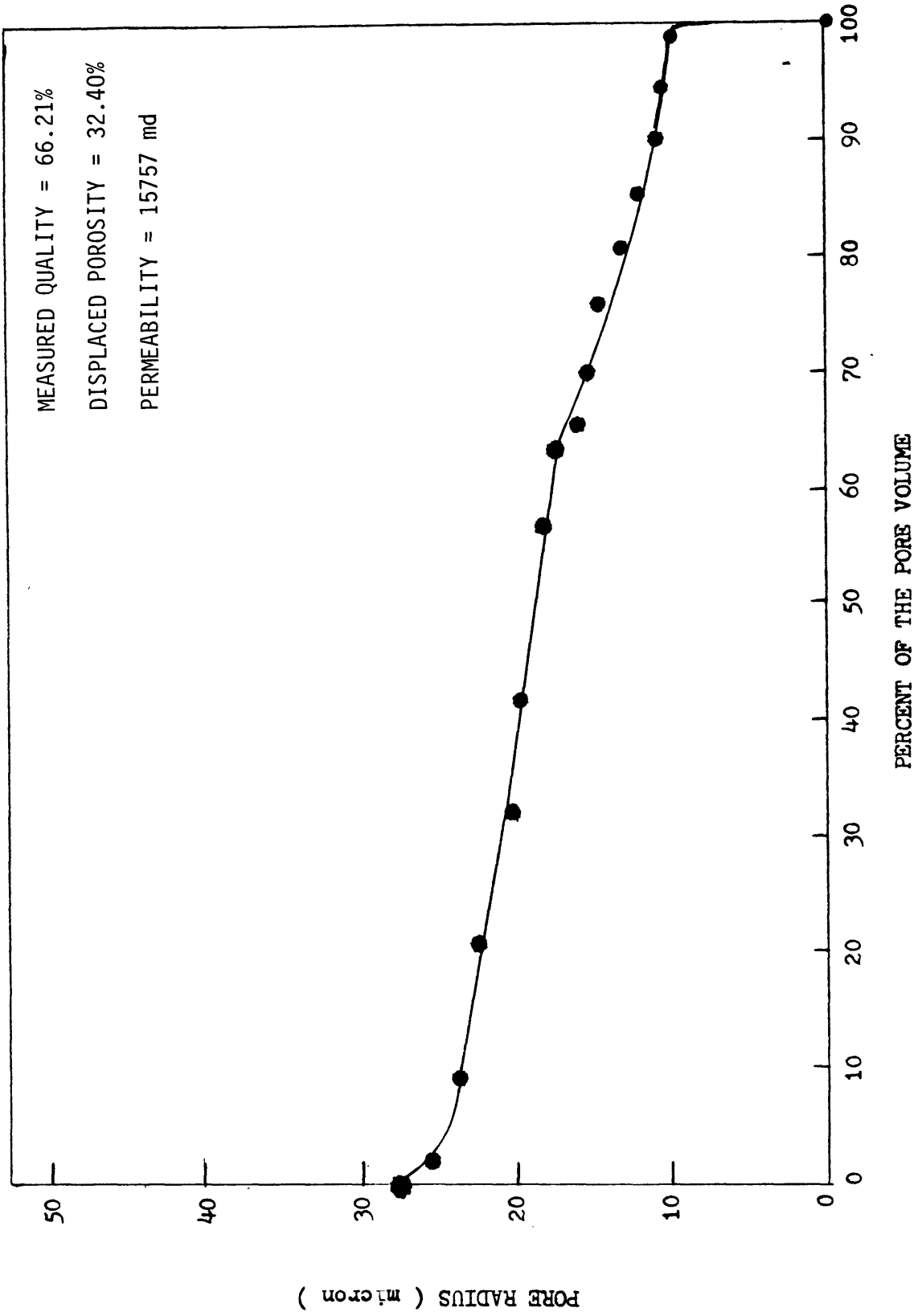


FIGURE 22: PORE SIZE DISTRIBUTION SAMPLE 2

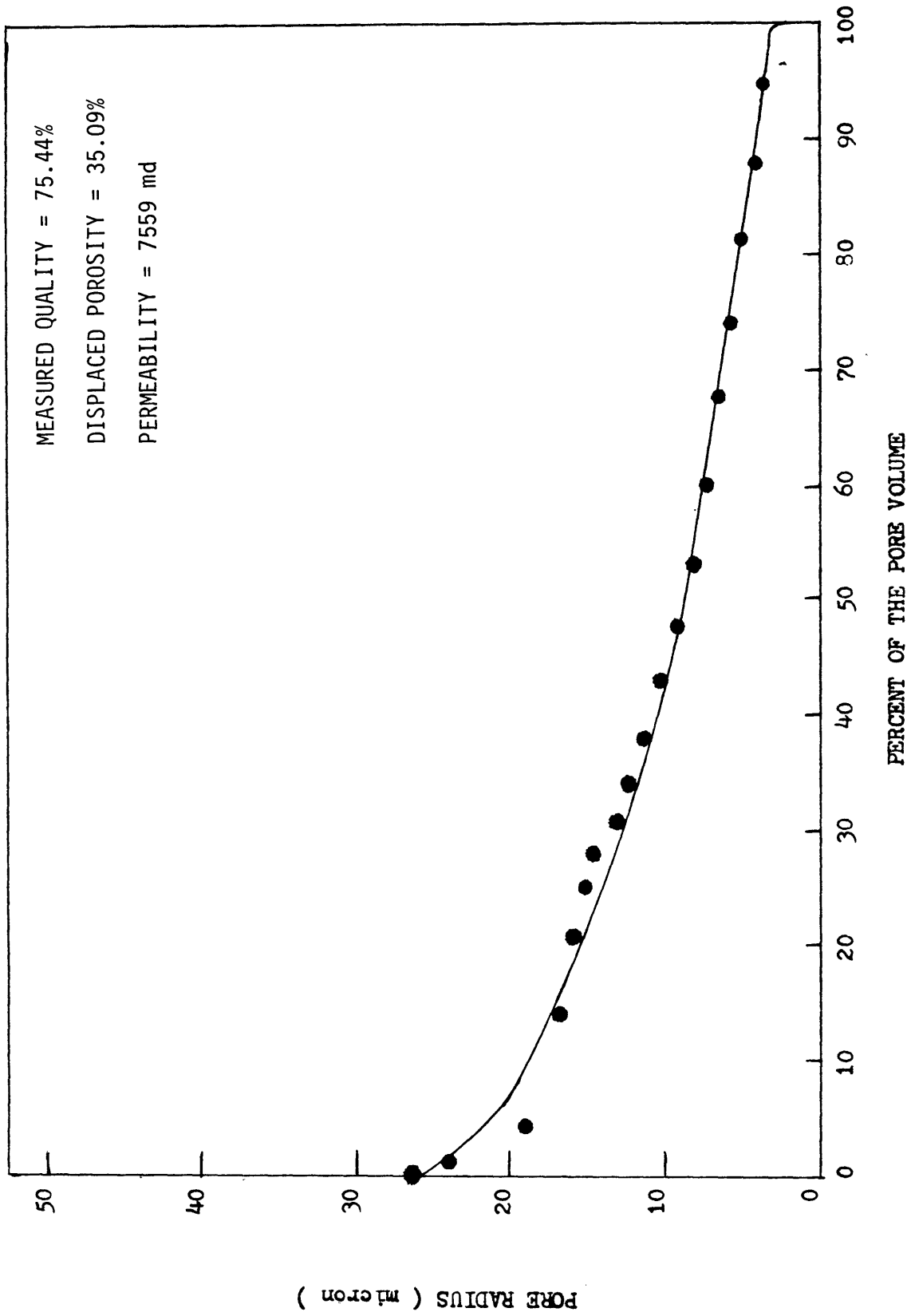


FIGURE 23: PORE SIZE DISTRIBUTION SAMPLE 3

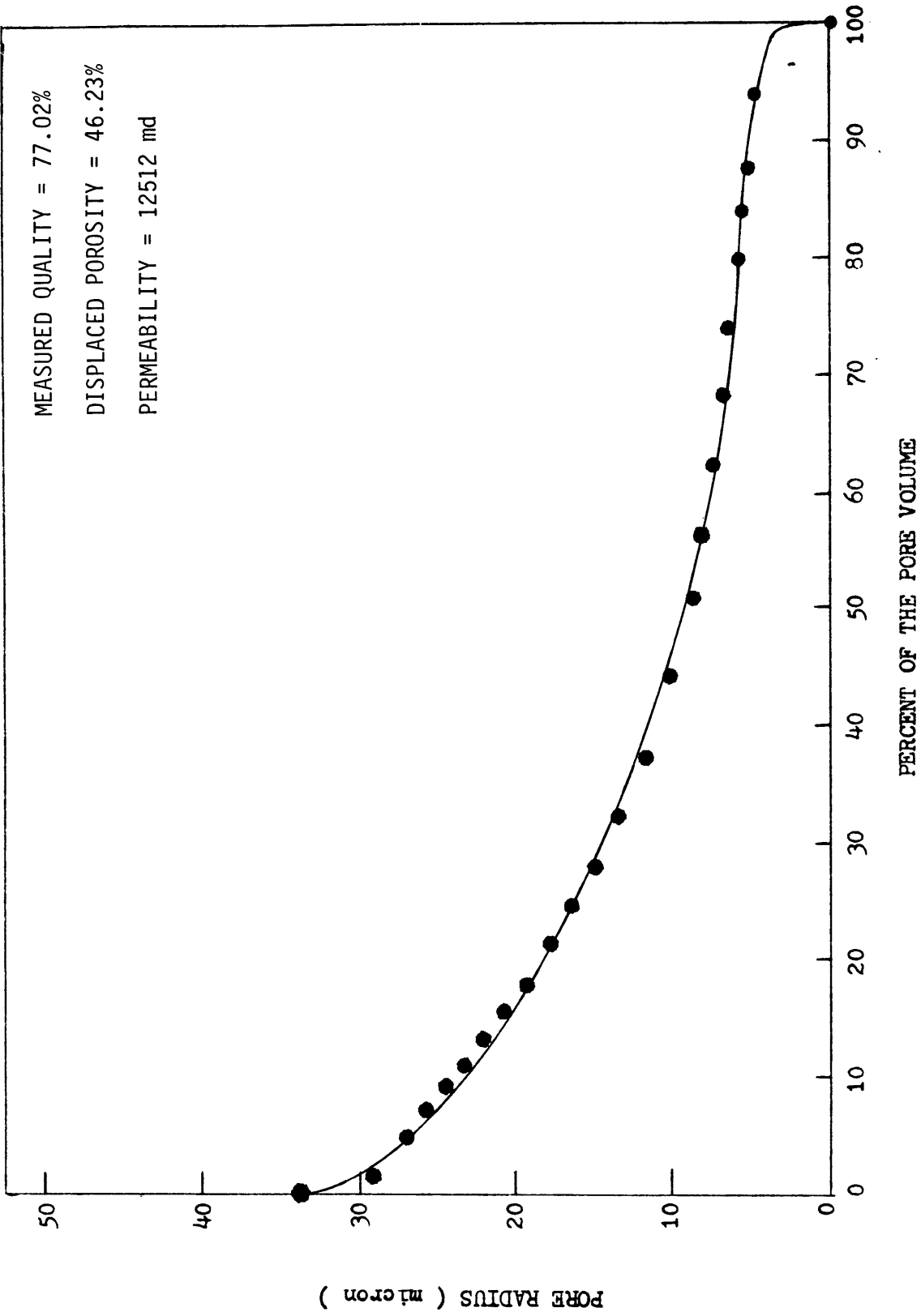


FIGURE 24: PORE SIZE DISTRIBUTION SAMPLE 4

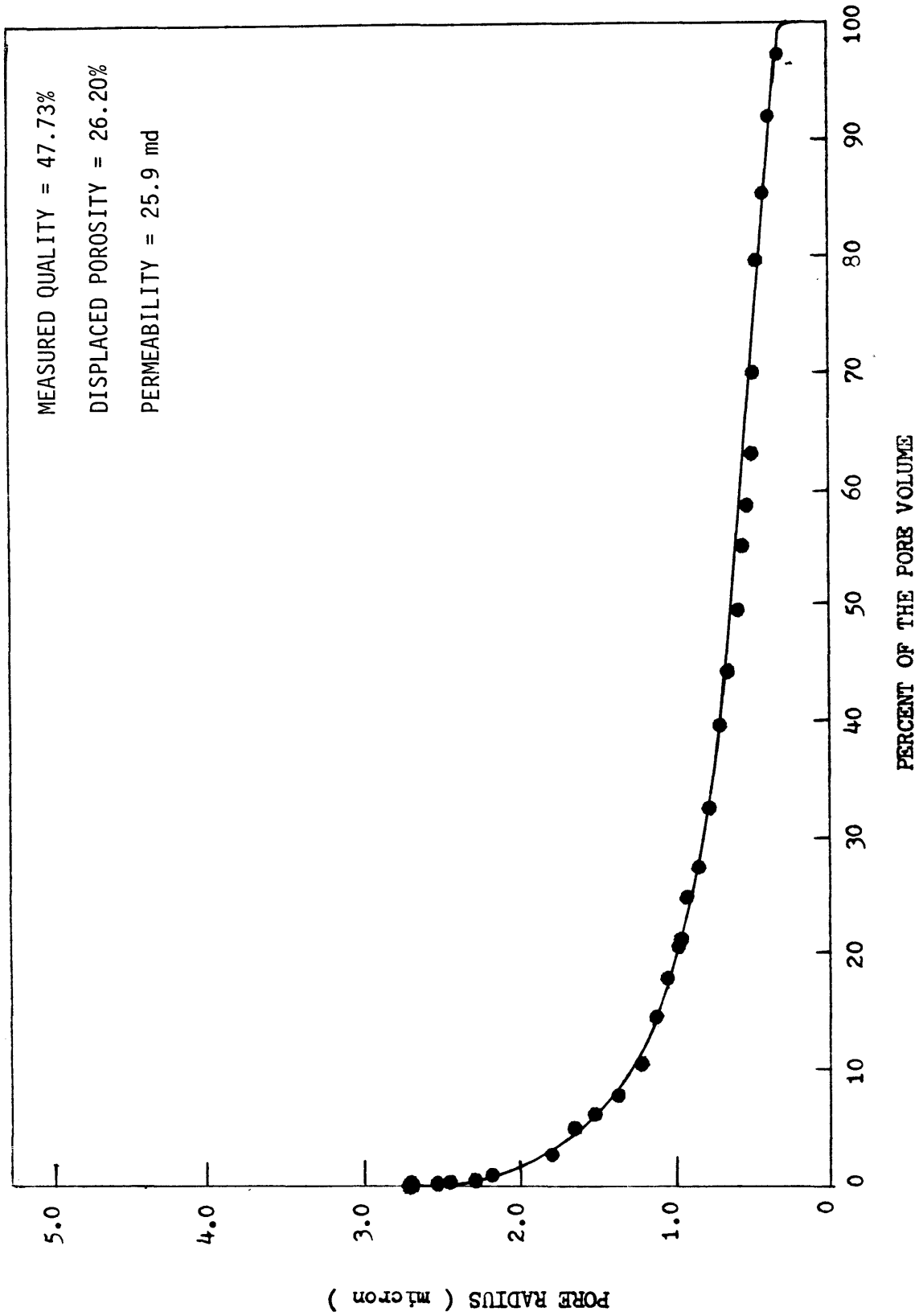


FIGURE 25: PORE SIZE DISTRIBUTION SAMPLE 5

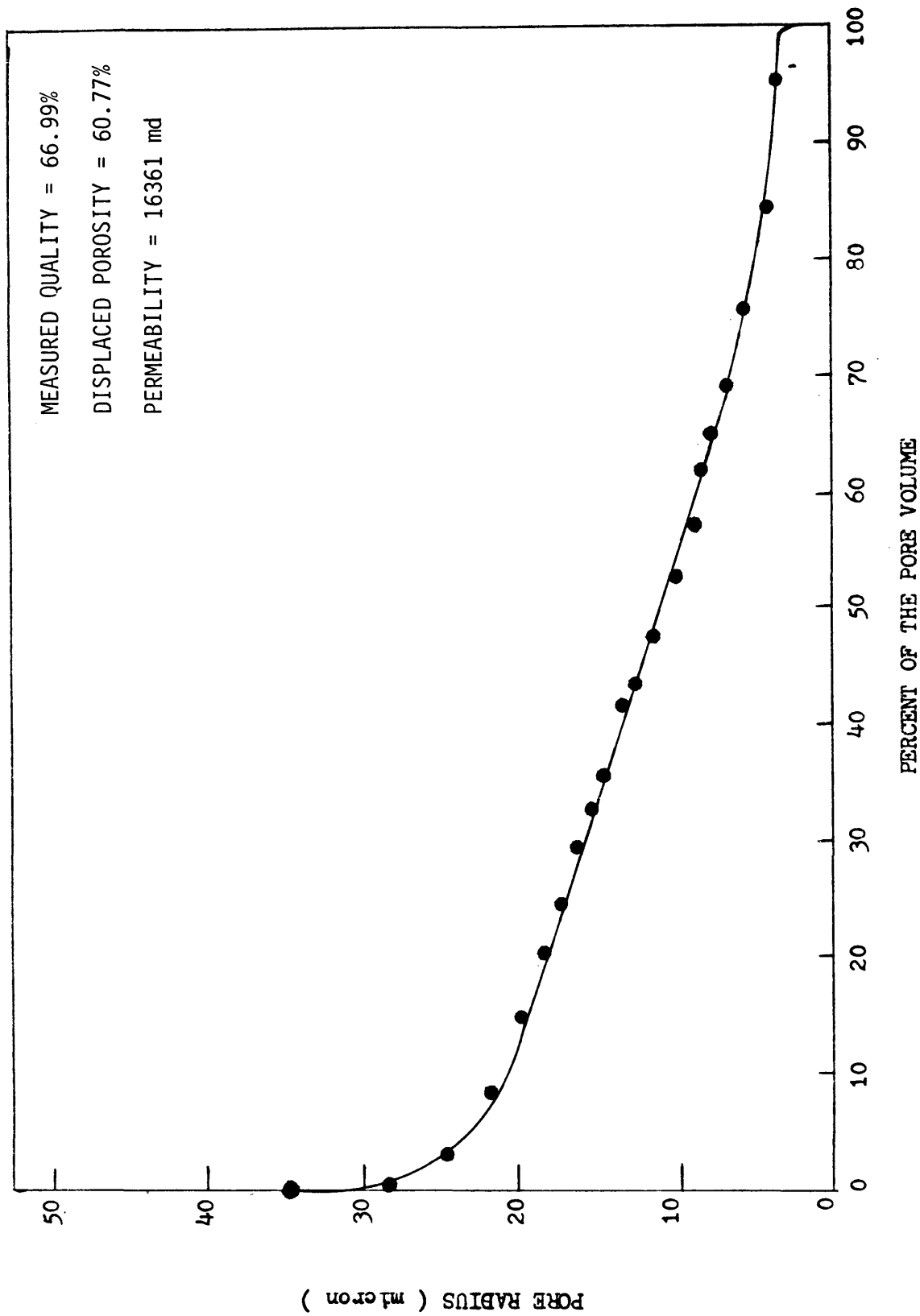


FIGURE 26: PORE SIZE DISTRIBUTION SAMPLE 6

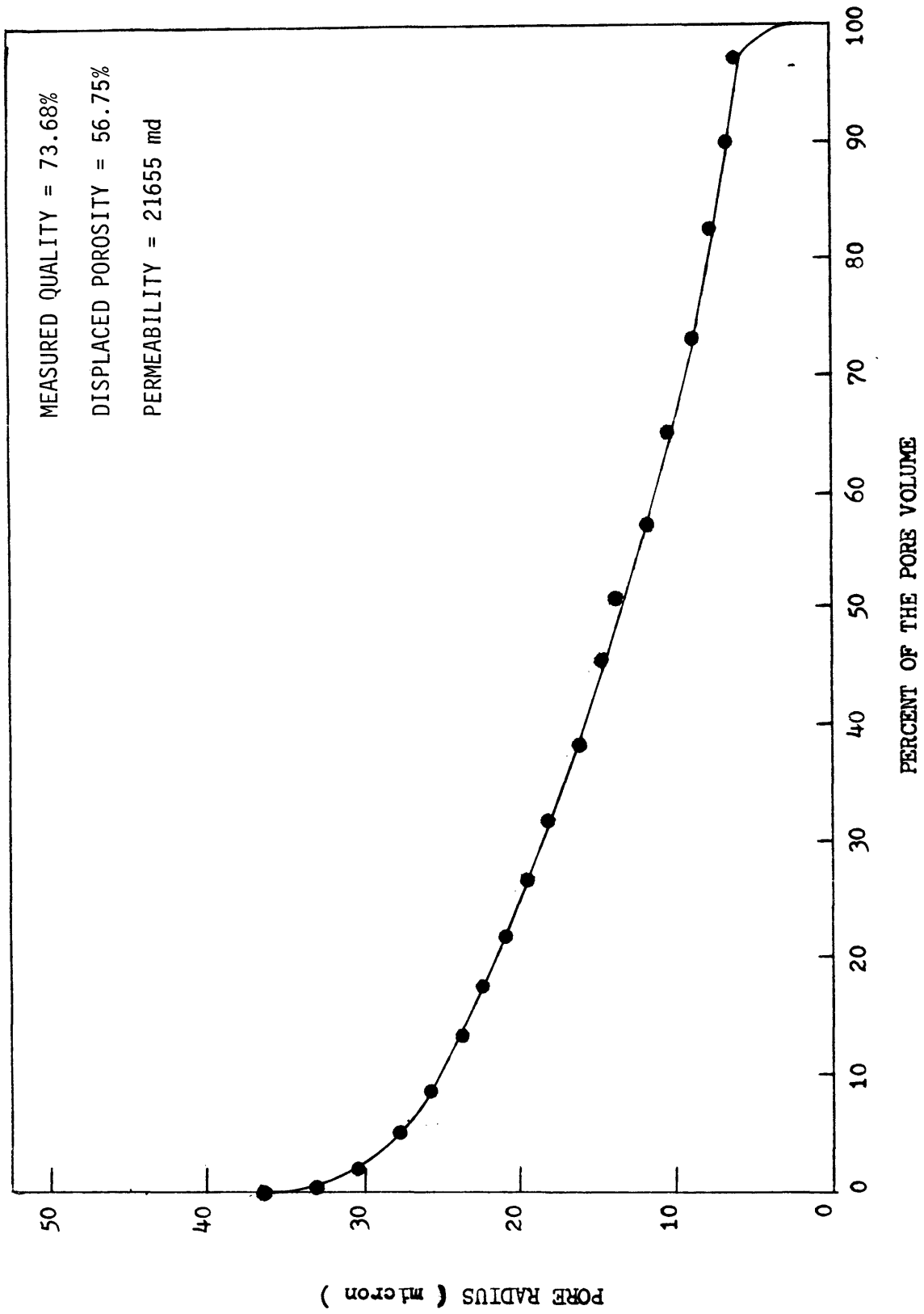


FIGURE 27: PORE SIZE DISTRIBUTION SAMPLE 7

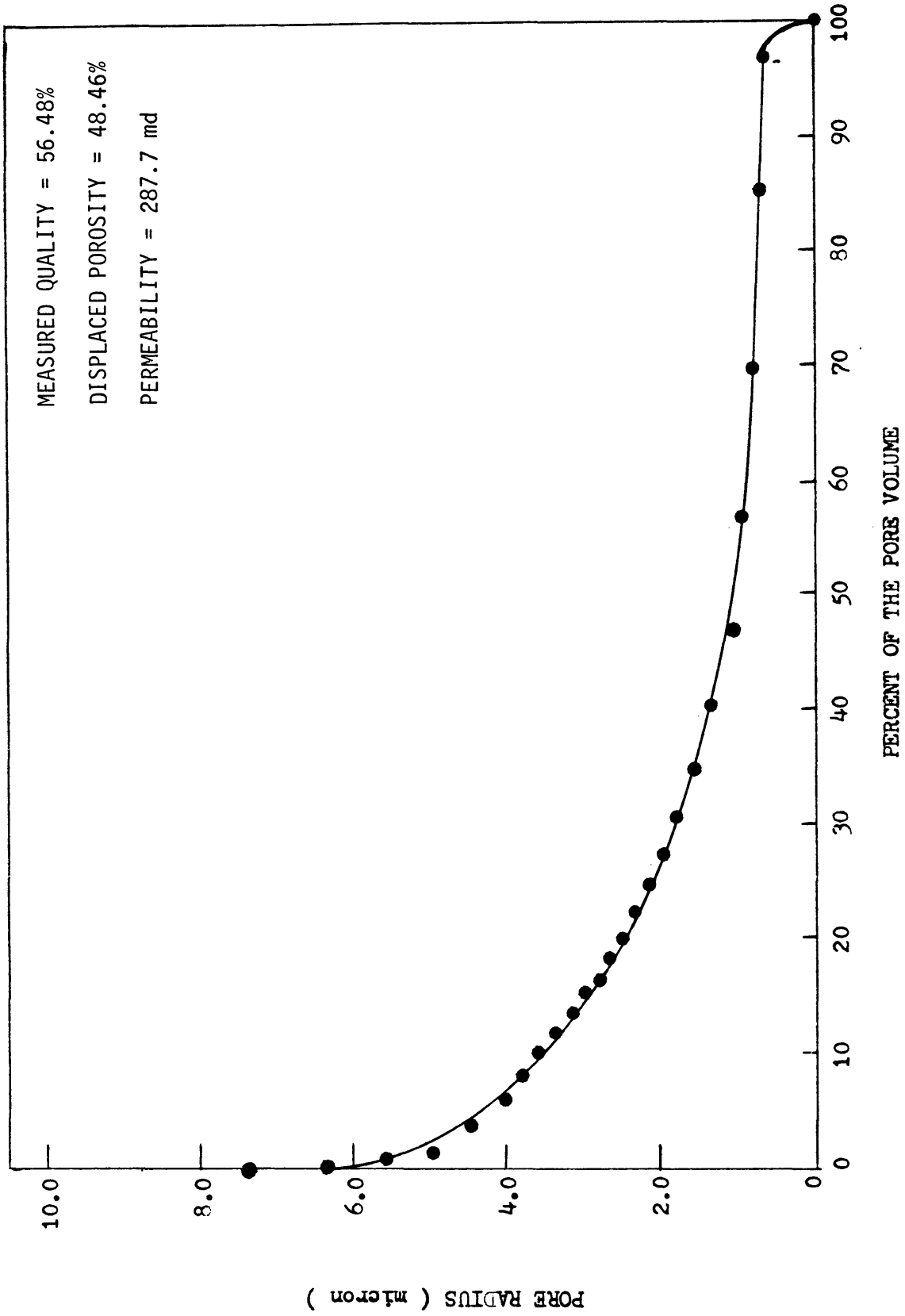


FIGURE 28: PORE SIZE DISTRIBUTION SAMPLE 8

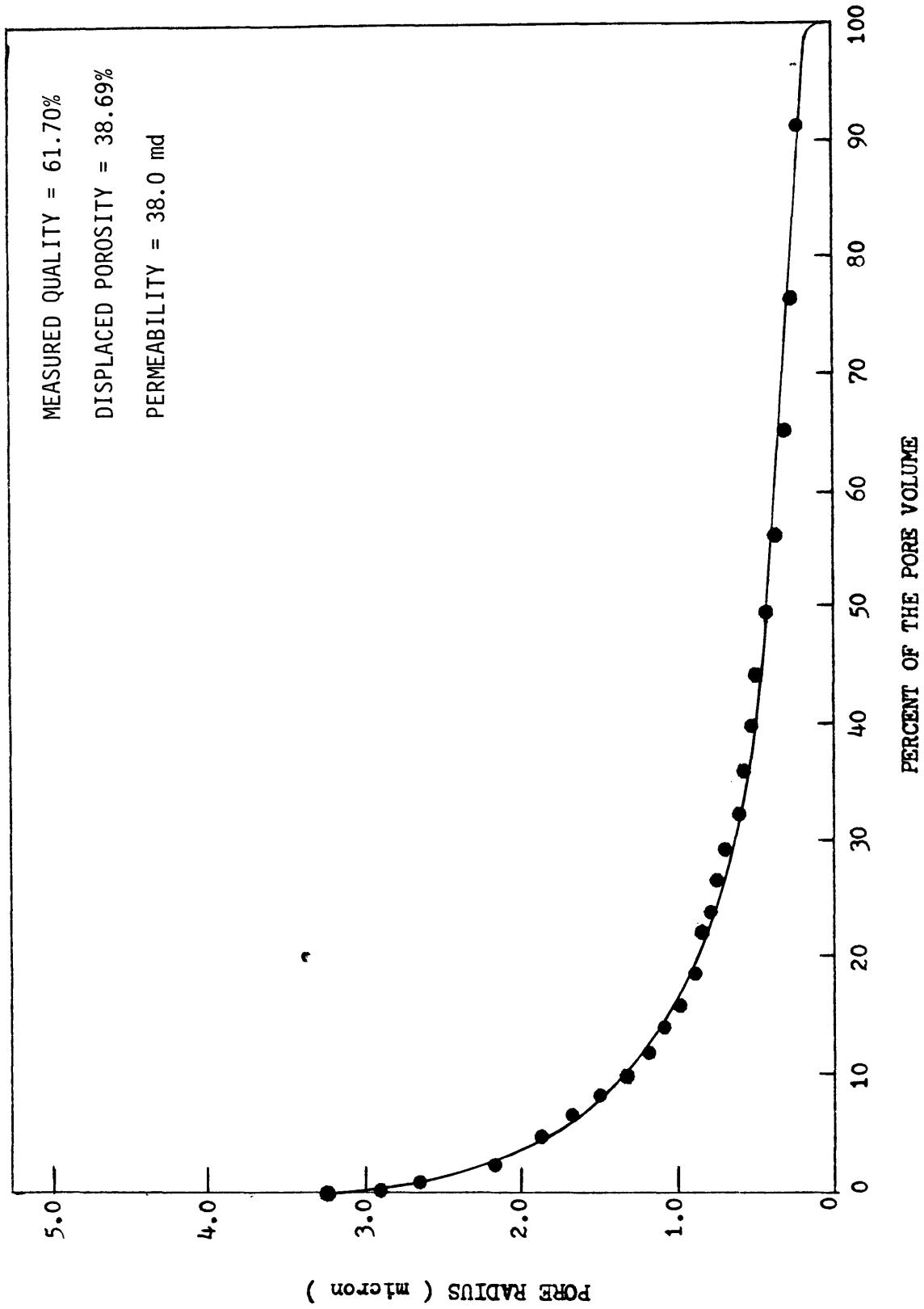


FIGURE 29: PORE SIZE DISTRIBUTION SAMPLE 9

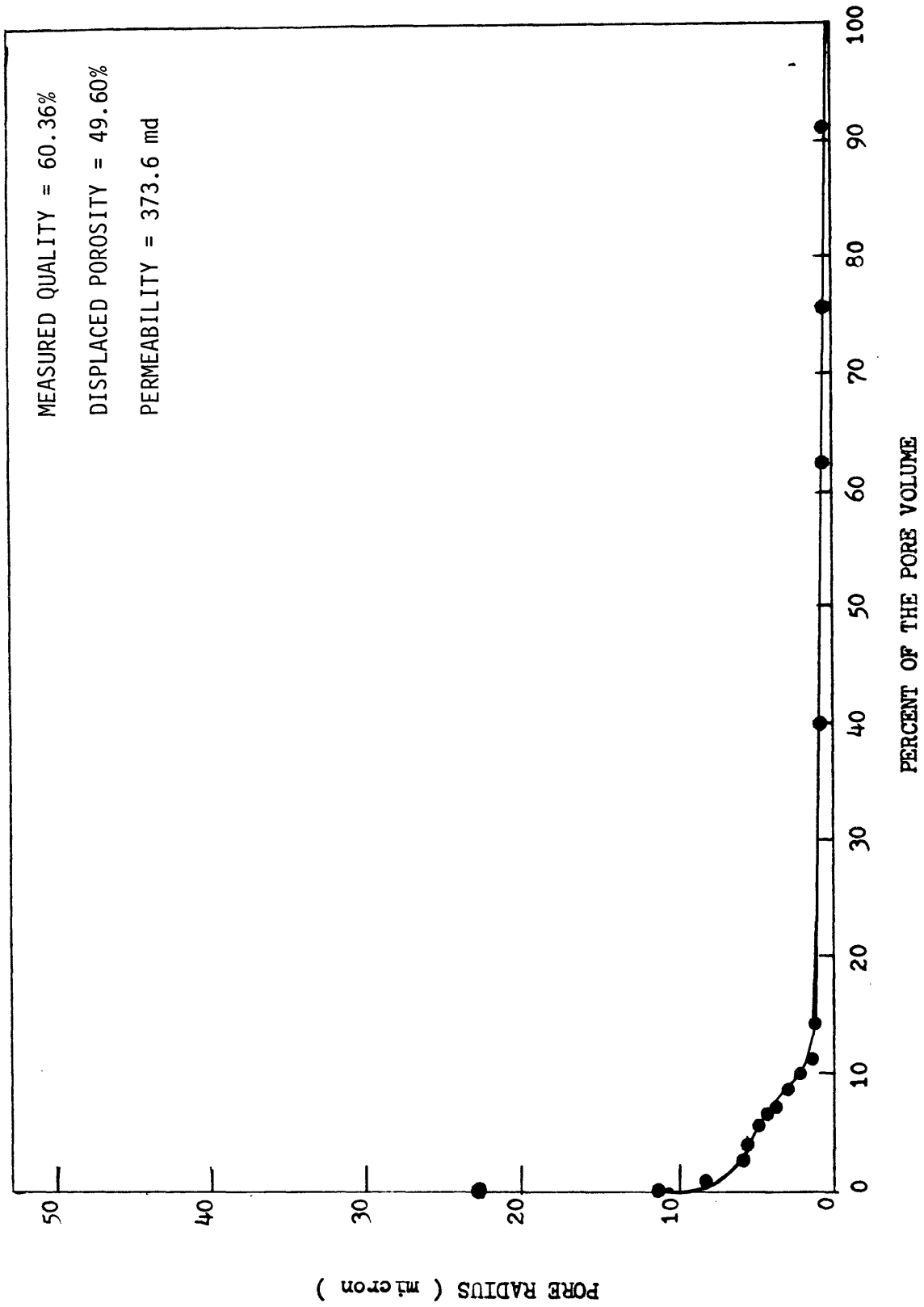


FIGURE 30: PORE SIZE DISTRIBUTION SAMPLE 10

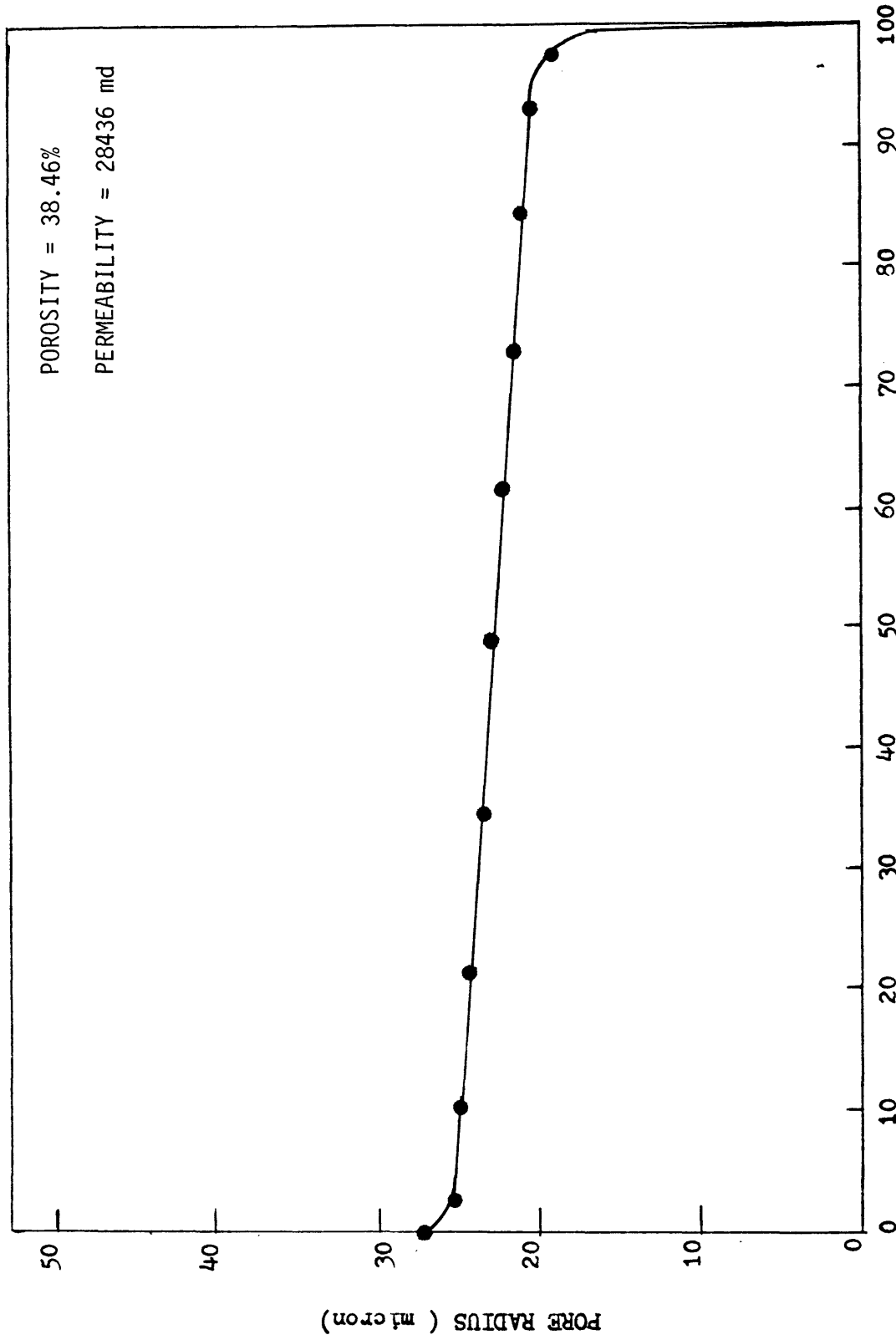
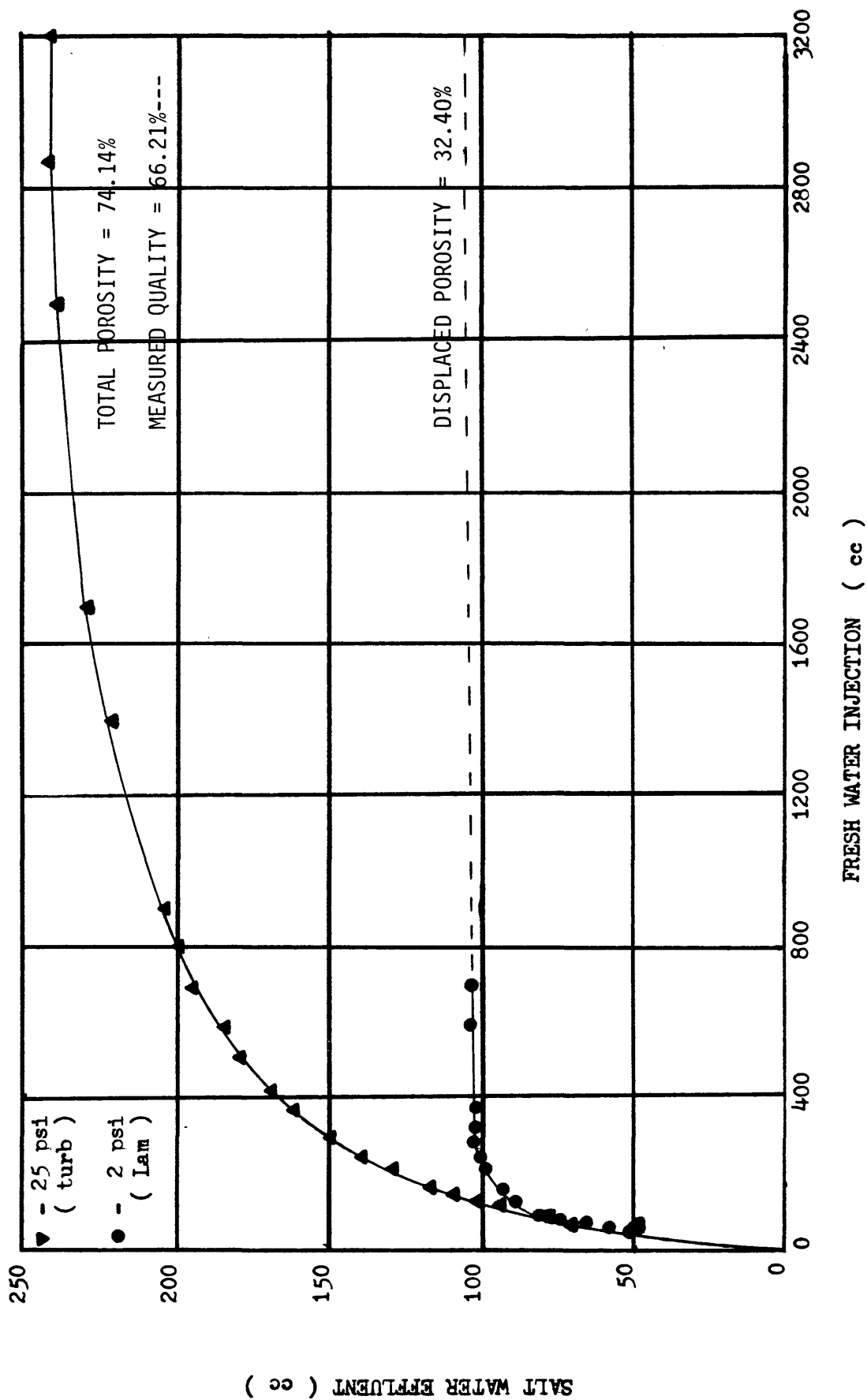


FIGURE 31: PORE SIZE DISTRIBUTION ANALYSIS
20 - 40 MESH SANDPACK

FIGURE 32
SAMPLE 2
MISCIBLE DISPLACEMENT IN TURBULENT AND LAMINAR FLOW REGIMES



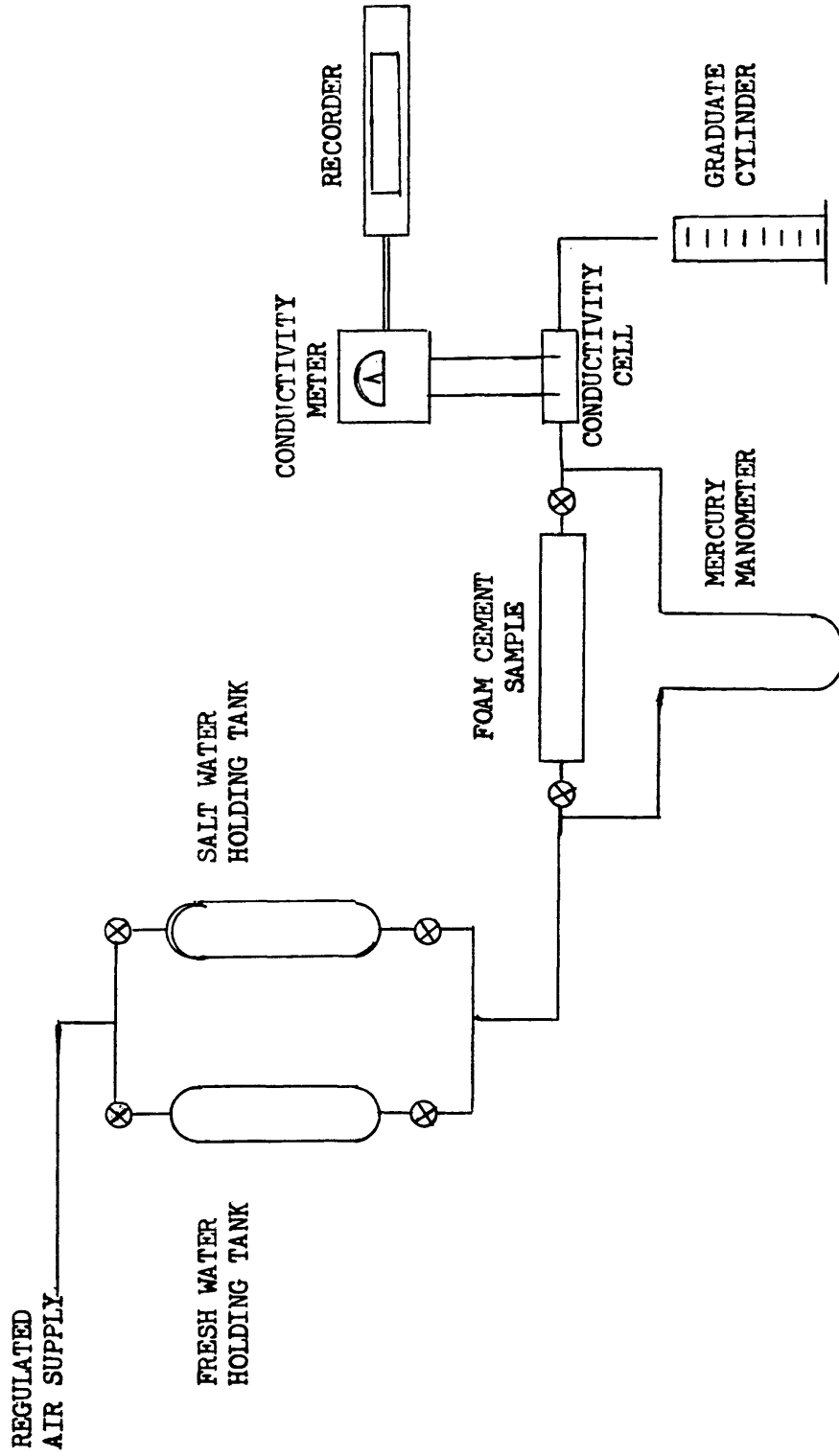


FIGURE 33 : SCHEMATIC DIAGRAM OF TEST APPARATUS

TABLE 1
SURFACE TENSION
ADOFOAM BF-1
IN TAP WATER

CONCENTRATION ADOFOAM BF-1 <u>% BY VOLUME</u>	SURFACE TENSION DYNES <u>PER CM</u>
0.000	72.2
0.002	62.5
0.020	43.4
0.096	33.6
0.192	33.2
0.200	32.9
0.640	34.5
2.000	36.5
3.200	37.4
10.000	36.3
16.000	36.7
20.000	35.5
40.000	33.6
80.000	31.2
100.000	30.8

TABLE 2

REPORT OF TESTS OF Class G PORTLAND CEMENT

ORRIER _____ Shipped _____

r _____ Quantity _____ Tons Silo A-12

assigned to _____ Test No. _____

Tests	%	Specification		Specification
	21.42		C ₃ S	45.1
	4.97		C ₂ S	27.5
	5.39		C ₃ A	4.1
	62.94		C ₄ AF	16.4
	1.00	Max.		
	2.53	Max.		
	0.95	Max.		
	0.22			
	0.47			
equiv.	0.53			
Residue	0.17	Max.		

Tests	Specification	Specification
Sq. Cm./Gm.		Setting Time
Air Perm.	3503	Initial Hrs. Min. 3:05
Turb.		Final Hrs. Min. 6:30
Volume Expansion %	-0.011	Entrained Air % 8.1
Compressive Strength P. S. I.		Tensile P. S. I.
1 day	1103	1 day
3 day	2367	3 day
7 day	3579	7 day
28 day	5792	28 day

Martin Marietta Cements comply with current Specifications of ASTM C150 _____

Federal SS-C-192 _____ and AASHO M85 _____

Prepared and sworn to
 on this _____ day of
 _____ 19 _____

MARTIN MARIETTA CORPORATION

 Quality Control Supervisor

 Notary Public

Commission Expires _____

TABLE 3
TEST DATA
SAMPLE 1

Bulk Volume: <u>366 cc</u>	Predicted Quality: <u>68.23%</u>
Length: <u>7.0 inches</u>	Measured Quality: <u>69.95%</u>
Diameter: <u>2.0 inches</u>	Total Pore Volume: <u>310 cc</u>
Water Ratio: <u>0.44 cc/gm</u>	Total Porosity: <u>84.70%</u>
Surfactant: <u>0.48%</u>	Displaced Pore Volume: <u>49 cc</u>
Setting Time: <u>72 hours</u>	Displaced Porosity: <u>13.50%</u>
Permeability: <u>19701 md</u>	Free Water: <u>54 cc</u>

TABLE 4
TEST DATA
SAMPLE 2

Bulk Volume: <u>321 cc</u>	Predicted Quality: <u>65.74%</u>
Length: <u>8.2 inches</u>	Measured Quality: <u>66.21%</u>
Diameter: <u>1.75 inches</u>	Total Pore Volume: <u>238 cc</u>
Water Ratio: <u>0.44 cc/gm</u>	Total Porosity: <u>74.14%</u>
Surfactant: <u>0.200%</u>	Displaced Pore Volume: <u>104 cc</u>
Setting Time: <u>72 hours</u>	Displaced Porosity: <u>32.40%</u>
Permeability: <u>15757 md</u>	Free Water: <u>25.5 cc</u>

TABLE 5
TEST DATA
SAMPLE 3

Bulk Volume: <u>171 cc</u>	Predicted Quality: <u>71.15%</u>
Length: <u>4.35 inches</u>	Measured Quality: <u>75.44%</u>
Diameter: <u>1.75 inches</u>	Total Pore Volume: <u>152 cc</u>
Water Ratio: <u>0.44 cc/gm</u>	Total Porosity: <u>88.89%</u>
Surfactant: <u>0.105%</u>	Displaced Pore Volume: <u>60 cc</u>
Setting Time: <u>72 hours</u>	Displaced Porosity: <u>35.09%</u>
Permeability: <u>7559 md</u>	Free Water: <u>23 cc</u>

TABLE 6
TEST DATA
SAMPLE 4

Bulk Volume: <u>235 cc</u>	Predicted Quality: <u>78.17%</u>
Length: <u>5.85 inches</u>	Measured Quality: <u>77.02%</u>
Diameter: <u>1.75 inches</u>	Total Pore Volume: <u>209 cc</u>
Water Ratio: <u>0.44 cc/gm</u>	Total Porosity: <u>88.94%</u>
Surfactant: <u>0.230%</u>	Displaced Pore Volume: <u>109 cc</u>
Setting Time: <u>72 hours</u>	Displaced Porosity: <u>46.23%</u>
Permeability: <u>12512 md</u>	Free Water: <u>28 cc</u>

TABLE 7
TEST DATA
SAMPLE 5

Bulk Volume: <u>220 cc</u>	Predicted Quality: <u>52.95%</u>
Length: <u>5.65 inches</u>	Measured Quality: <u>47.73%</u>
Diameter: <u>1.75 inches</u>	Total Pore Volume: <u>118 cc</u>
Water Ratio: <u>0.44 cc/gm</u>	Total Porosity: <u>53.64%</u>
Surfactant: <u>0.180%</u>	Displaced Pore Volume: <u>58 cc</u>
Setting Time: <u>72 hours</u>	Displaced Porosity: <u>26.20%</u>
Permeability: <u>25.9 md</u>	Free Water: <u>13 cc</u>

TABLE 8
TEST DATA
SAMPLE 6

Bulk Volume: <u>209 cc</u>	Predicted Quality: <u>67.13%</u>
Length: <u>5.1 inches</u>	Measured Quality: <u>66.99%</u>
Diameter: <u>1.75 inches</u>	Total Pore Volume: <u>167 cc</u>
Water Ratio: <u>0.44 cc/gm</u>	Total Porosity: <u>79.90%</u>
Surfactant: <u>0.545%</u>	Displaced Pore Volume: <u>127 cc</u>
Setting Time: <u>72 hours</u>	Displaced Porosity: <u>60.77%</u>
Permeability: <u>16361 md</u>	Free Water: <u>27 cc</u>

TABLE 9
TEST DATA
SAMPLE 7

Bulk Volume: <u>209 cc</u>	Predicted Quality: <u>71.24%</u>
Length: <u>5.10 inches</u>	Measured Quality: <u>73.68%</u>
Diameter: <u>1.75 inches</u>	Total Pore Volume: <u>168 cc</u>
Water Ratio: <u>0.44 cc/gm</u>	Total Porosity: <u>80.38%</u>
Surfactant: <u>0.187%</u>	Displaced Pore Volume: <u>119 cc</u>
Setting Time: <u>72 hours</u>	Displaced Porosity: <u>56.75%</u>
Permeability: <u>21655 md</u>	Free Water: <u>14 cc</u>

TABLE 10
TEST DATA
SAMPLE 8

Bulk Volume: <u>324 cc</u>	Predicted Quality: <u>57.48%</u>
Length: <u>8.2 inches</u>	Measured Quality: <u>56.48%</u>
Diameter: <u>1.75 inches</u>	Total Pore Volume: <u>235 cc</u>
Water Ratio: <u>0.44 cc/gm</u>	Total Porosity: <u>72.53%</u>
Surfactant: <u>0.148%</u>	Displaced Pore Volume: <u>157 cc</u>
Setting Time: <u>48 hours</u>	Displaced Porosity: <u>48.46%</u>
Permeability: <u>287.7 md</u>	Free Water: <u>52 cc</u>

TABLE 11
TEST DATA
SAMPLE 9

Bulk Volume: <u>235 cc</u>	Predicted Quality: <u>61.37%</u>
Length: <u>6.0 inches</u>	Measured Quality: <u>61.70%</u>
Diameter: <u>1.75 inches</u>	Total Pore Volume: <u>160 cc</u>
Water Ratio: <u>0.44 cc/gm</u>	Total Porosity: <u>68.09%</u>
Surfactant: <u>0.187%</u>	Displaced Pore Volume: <u>91 cc</u>
Setting Time: <u>48 hours</u>	Displaced Porosity: <u>38.69%</u>
Permeability: <u>38.0 md</u>	Free Water: <u>15 cc</u>

TABLE 12
TEST DATA
SAMPLE 10

Bulk Volume: <u>169 cc</u>	Predicted Quality: <u>60.50%</u>
Length: <u>4.3 inches</u>	Measured Quality: <u>60.36%</u>
Diameter: <u>1.75 inches</u>	Total Pore Volume: <u>114 cc</u>
Water Ratio: <u>0.44 cc/gm</u>	Total Porosity: <u>67.46%</u>
Surfactant: <u>0.187%</u>	Displaced Pore Volume: <u>84 cc</u>
Setting Time: <u>48 hours</u>	Displaced Porosity: <u>49.60%</u>
Permeability: <u>373.6 md</u>	Free Water: <u>12.0 cc</u>

TABLE 13
TEST DATA
SAMPLE 11

Bulk Volume: <u>200 cc</u>	Predicted Quality: <u>55.45%</u>
Length: <u>5.1 inches</u>	Measured Quality: <u>48.00%</u>
Diameter: <u>1.75 inches</u>	Surfactant: <u>0.162%</u>
Water Ratio: <u>0.44 cc/gm</u>	Permeability: <u>0.0 md</u>
Setting Time: <u>72 hours</u>	

TABLE 14
TEST DATA
SAMPLE 12

Bulk Volume: <u>244 cc</u>	Predicted Quality: <u>53.11%</u>
Length: <u>6.15 inches</u>	Measured Quality: <u>41.80%</u>
Diameter: <u>1.75 inches</u>	Surfactant: <u>0.116%</u>
Water Ratio: <u>0.44 cc/gm</u>	Permeability: <u>0.0 md</u>
Setting Time: <u>72 hours</u>	

TABLE 15
TEST DATA
SAMPLE 13

Bulk Volume: <u>328 cc</u>	Setting Time: <u>19 days</u>
Length: <u>6.3 inches</u>	Predicted Quality: <u>59.17%</u>
Diameter: <u>2.0 inches</u>	Measured Quality: <u>63.88%</u>
Water Ratio: <u>0.44 cc/gm</u>	Permeability: <u>1875 md*</u>
Surfactant: <u>0.142%</u>	

* Tests were conducted with kerosene with a viscosity of 2.7 cp and density of 0.81 gm/cc.

TABLE 16
TEST DATA
20-40 MESH SAND

Bulk Volume: <u>260 cc</u>	Pore Volume: <u>100 cc</u>
Length: <u>6.5 inches</u>	Porosity: <u>38.46%</u>
Diameter: <u>1.75 inches</u>	Permeability: <u>28.436 darcies</u>

TABLE 17
 FILTER LOSS OF FOAM CEMENT

<u>Quality</u> <u>(%)</u>	<u>Water</u> <u>Loss</u> <u>@ 30 sec</u>	<u>Foam</u> <u>Loss</u> <u>@ 30 sec</u>	<u>Water</u> <u>Loss</u> <u>@ 60 sec</u>	<u>Foam</u> <u>Loss</u> <u>@ 60 sec</u>	<u>Time to</u> <u>Dehydrate</u> <u>(sec)</u>
0.00	45	45	57	57	70
0.00	42	42	60	60	105
38.32	27	30	41	48	65
38.84	27	35	-	-	35
46.75	25	34	37	47	110
55.19	25	39	36	49	95
69.68	24	57	35	77	80
88.93	20	68	31	103	75

Tests conducted with standard A.P.I. mud filter press at room temperature and 50 psig.

TABLE 18
 INTERACTION OF FOAM CEMENT
 WITH 20 - 40 MESH SAND

	<u>TEST #1</u>	<u>TEST #2</u>	<u>TEST #3</u>
Tube Length (inches)	7.4	6.2	5.7
Sand Length (inches)	3.4	3.5	2.6
Upstream Pressure (psia)	37.0	37.0	37.0
Downstream Pressure (psia)	12.0	27.0	32.0
Quality of Cement Slurry @ 37 psia	70.8%	67.47%	73.1%
Sand Porosity (%)	31.0	37.2	41.6
Final Length of Cement Plug (inches)	2.0	1.8	1.0
Average Quality* of Cement Plug (%)	22.1%	18.1%	26.2%

*-The average quality was determined from the weight of the dry cement and the dimensions of the plug. It was assumed that the density ratio of wet to dry cement was 1.205.

TABLE 19
DIFFERENTIAL PRESSURE
VERSUS WATER FLOW RATE
SAMPLE 1

<u>Pressure</u> <u>(psi)</u>	<u>Flow Rate</u> <u>(cc/min)</u>
0.68	63
0.75	72
0.95	89
1.15	104
1.35	112
1.50	146
1.60	148
1.90	181
2.10	200
2.50	233
2.85	264
3.30	297
3.95	340
5.65	431
7.50	495
11.30	547

TABLE 20
DIFFERENTIAL PRESSURE
VERSUS WATER FLOW RATE
SAMPLE 2

<u>Pressure</u> <u>(psi)</u>	<u>Flow Rate</u> <u>(cc/min)</u>
1.75	83
2.25	100
2.75	134
3.25	157
3.75	181
4.25	206
5.25	250
6.25	285
8.75	360
11.25	418
13.25	468
14.25	490

TABLE 21
DIFFERENTIAL PRESSURE
VERSUS WATER FLOW RATE
SAMPLE 3

<u>Pressure</u> <u>(psi)</u>	<u>Flow Rate</u> <u>(cc/min)</u>
0.50	20
1.15	51
1.50	65
1.73	76
2.00	85
2.20	94
2.65	114
3.10	129
3.70	147
4.00	165
4.90	197
6.00	231
6.70	251
7.25	276
8.50	304

TABLE 22
DIFFERENTIAL PRESSURE
VERSUS WATER FLOW RATE
SAMPLE 4

<u>Pressure</u> <u>(psi)</u>	<u>Flow Rate</u> <u>(cc/min)</u>
1.00	54
1.30	69
1.50	79
1.75	94
1.98	105
2.23	120
2.65	138
3.10	156
3.50	175
4.10	193
4.30	211
4.80	231
5.70	264
6.50	298
7.40	328
8.30	369

TABLE 23
DIFFERENTIAL PRESSURE
VERSUS WATER FLOW RATE
SAMPLE 5

<u>Pressure</u> <u>(psi)</u>	<u>Flow Rate</u> <u>(cc/min)</u>
2.0	0.23
2.8	0.30
3.5	0.40
4.2	0.50
5.0	0.56
6.0	0.65
7.5	0.85
9.0	1.10
11.0	1.25
12.0	1.38
13.5	1.55
15.0	1.70
16.0	1.80
17.0	1.93

TABLE 24
DIFFERENTIAL PRESSURE
VERSUS WATER FLOW RATE
SAMPLE 6

<u>Pressure</u> <u>(psi)</u>	<u>Flow Rate</u> <u>(cc/min)</u>
0.50	40
1.00	75
1.50	120
2.00	155
2.50	200
3.00	240
3.75	300
4.25	345
4.75	380
5.25	415
6.25	480
7.25	545
8.75	630

TABLE 25
DIFFERENTIAL PRESSURE
VERSUS WATER FLOW RATE
SAMPLE 7

<u>Pressure</u> <u>(psi)</u>	<u>Flow Rate</u> <u>(cc/min)</u>
1.00	100
1.25	124
1.70	167
2.05	205
2.30	232
2.50	250
2.75	276
3.20	322
3.70	365
4.40	410
5.30	481
7.65	622

TABLE 26
DIFFERENTIAL PRESSURE
VERSUS WATER FLOW RATE
SAMPLE 8

<u>Pressure</u> <u>(psi)</u>	<u>Flow Rate</u> <u>(cc/min)</u>
1.00	0.90
2.10	1.80
3.00	2.70
4.00	3.50
5.00	4.40
6.00	5.20
7.00	6.00
8.20	7.20
9.40	8.30
10.60	9.20
12.10	10.70
13.50	11.60

TABLE 27
DIFFERENTIAL PRESSURE
VERSUS WATER FLOW RATE
SAMPLE 9

Pressure <u>(psi)</u>	Flow Rate <u>(cc/min)</u>
3.0	0.50
4.0	0.65
5.0	0.80
6.0	0.95
7.0	1.10
8.0	1.25
10.1	1.60
12.4	1.95
14.6	2.30
17.0	2.60
22.2	3.50

TABLE 28
DIFFERENTIAL PRESSURE
VERSUS WATER FLOW RATE
SAMPLE 10

<u>Pressure</u> <u>(psi)</u>	<u>Flow Rate</u> <u>(cc/min)</u>
1.0	2.0
3.0	7.0
4.2	9.0
5.8	12.5
7.0	15.0
8.0	17.0
9.7	22.0
11.2	24.0
13.5	29.0
15.6	34.0
17.2	37.0

TABLE 29
DIFFERENTIAL PRESSURE
VERSUS KEROSENE FLOW RATE
SAMPLE 13

<u>Pressure</u> <u>(psi)</u>	<u>Flow Rate</u> <u>(cc/min)</u>
2.0	7.5
3.0	10.5
4.0	14.5
5.0	18.0
6.0	21.5
7.0	24.0
8.0	26.5
9.0	30.0
10.0	32.0
11.0	35.5
12.0	37.5

TABLE 30
DIFFERENTIAL PRESSURE
VERSUS WATER FLOW RATE
20 - 40 MESH SAND

<u>Pressure</u> <u>(psi)</u>	<u>Flow Rate</u> <u>(cc/min)</u>
1.00	110
1.20	130
1.40	150
1.60	178
1.80	195
2.00	220
2.50	270
3.00	330
3.50	385
3.80	415
4.60	460
5.30	520
6.40	580

TABLE 31
PORE SIZE DISTRIBUTION
SAMPLE NUMBER 1

Fresh Water Injection <u>(cc)</u>	Salt Water Effluent <u>(cc)</u>	$\frac{dR}{dV}$ <u> </u>	S <u>(%)</u>	Pore Radius <u>(micron)</u>
6.193	6.193	1.0000	0.00	95.88
9.290	9.140	0.9517	0.64	78.28
13.418	12.500	0.8138	3.40	65.14
17.547	15.233	0.6620	7.77	56.96
20.643	16.963	0.5587	11.67	52.51
24.772	18.928	0.4759	15.34	47.94
27.869	20.188	0.4069	19.01	45.20
30.965	21.298	0.3585	21.91	42.88
35.094	22.608	0.3173	24.65	40.28
40.255	24.302	0.2759	27.77	37.61
47.480	25.706	0.2345	31.36	34.63
54.705	27.171	0.2000	34.87	32.26
65.027	28.951	0.1725	38.11	29.59
77.413	30.744	0.1448	41.96	27.12
94.960	32.802	0.1172	46.56	24.48
122.829	35.300	0.0897	52.17	21.53
147.600	37.009	0.0689	57.65	19.64

(Continued)

TABLE 31
PORE SIZE DISTRIBUTION
SAMPLE NUMBER 1

Fresh Water Injection <u>(cc)</u>	Salt Water Effluent <u>(cc)</u>	$\frac{dR}{dV}$ <u> </u>	S <u>(%)</u>	Pore Radius <u>(micron)</u>
175.470	38.546	0.0551	62.10	18.01
230.174	40.810	0.0414	67.21	15.73
323.070	43.373	0.0276	74.04	13.27
505.764	45.893	0.0138	83.61	10.61
694.652	46.544	0.0035	94.86	9.05
770.000	46.544	0.0000	100.00	0.00

TABLE 32
PORE SIZE DISTRIBUTION
SAMPLE NUMBER 2

Fresh Water Injection <u>(cc)</u>	Salt Water Effluent <u>(cc)</u>	$\frac{dR}{dV}$ <u> </u>	S <u>(%)</u>	Pore Radius <u>(micron)</u>
52.352	52.352	1.0000	0.00	27.62
61.378	60.963	0.9530	2.35	25.51
70.404	68.421	0.8267	9.82	23.82
79.430	74.368	0.6600	21.10	22.42
88.456	79.000	0.5133	32.30	21.25
97.482	82.678	0.4067	41.38	20.24
106.508	85.632	0.3267	48.88	19.36
115.534	88.028	0.2667	57.00	18.59
124.561	90.022	0.2200	63.27	17.91
142.613	93.215	0.1767	65.40	16.73
160.665	95.683	0.1367	70.89	15.77
178.717	97.544	0.1033	76.04	14.95
214.822	100.190	0.0733	81.19	13.63
250.926	101.488	0.0500	85.52	12.62
287.031	103.204	0.0333	90.03	11.80
323.135	103.807	0.0167	94.63	11.12
380.000	104.000	0.0033	98.78	10.25
500.000	104.000	0.0000	100.00	0.00

TABLE 33
PORE SIZE DISTRIBUTION
SAMPLE NUMBER 3

Fresh Water Injection <u>(cc)</u>	Salt Water Effluent <u>(cc)</u>	$\frac{dR}{dV}$ <u> </u>	S <u>(%)</u>	Pore Radius <u>(micron)</u>
14.866	14.407	0.9691	0.00	26.20
17.840	17.142	0.9199	1.23	23.92
27.750	24.192	0.7840	4.08	19.18
35.184	29.317	0.5926	14.19	17.03
40.139	31.687	0.4785	20.92	15.95
43.608	33.133	0.4166	25.08	15.30
47.077	34.439	0.3765	28.01	14.72
51.537	35.953	0.3395	30.93	13.32
57.483	37.752	0.3027	34.11	12.40
66.403	40.064	0.2593	38.29	11.56
76.314	42.205	0.2160	43.10	10.64
90.189	44.690	0.1790	47.84	9.63
110.011	47.503	0.1420	53.43	8.43
143.708	51.043	0.1049	60.27	7.62
175.918	53.431	0.0741	67.71	6.88
215.561	55.512	0.0525	74.08	6.12
272.549	57.443	0.0340	80.76	5.40

(Continued)

TABLE 33
 PORE SIZE DISTRIBUTION
 SAMPLE NUMBER 3

Fresh Water Injection <u>(cc)</u>	Salt Water Effluent <u>(cc)</u>	$\frac{dR}{dV}$ <u> </u>	S <u>(%)</u>	Pore Radius <u>(micron)</u>
349.358	58.861	0.0285	87.81	4.62
478.000	59.668	0.0062	95.05	4.31
556.000	59.668	0.0000	100.00	0.00

TABLE 34
 PORE SIZE DISTRIBUTION
 SAMPLE NUMBER 4

<u>Fresh</u> <u>Water</u> <u>Injection</u> <u>(cc)</u>	<u>Salt</u> <u>Water</u> <u>Effluent</u> <u>(cc)</u>	<u>$\frac{dR}{dV}$</u>	<u>S</u> <u>(%)</u>	<u>Pore</u> <u>Radius</u> <u>(micron)</u>
20.41	20.41	1.0000	0.00	33.73
27.33	26.71	0.9105	1.68	29.14
31.48	29.93	0.7756	5.08	27.16
34.94	32.35	0.6995	7.28	25.78
38.40	34.56	0.6388	9.23	24.59
42.55	37.00	0.5853	11.13	23.36
47.40	39.55	0.5306	13.25	22.13
53.62	42.51	0.4753	15.67	20.81
61.93	46.01	0.4203	18.39	19.36
73.69	50.32	0.3664	21.46	17.75
86.14	54.26	0.3172	24.80	16.42
103.44	58.99	0.2734	28.26	14.98
127.66	64.55	0.2296	32.44	13.49
167.10	71.87	0.1859	37.57	11.79
222.45	79.74	0.1420	44.32	10.22
270.88	85.03	0.1092	51.03	9.26
333.16	90.48	0.0874	56.50	8.35

(Continued)

TABLE 34
PORE SIZE DISTRIBUTION
SAMPLE NUMBER 4

Fresh Water Injection <u>(cc)</u>	Salt Water Effluent <u>(cc)</u>	$\frac{dR}{dV}$ <u> </u>	S <u>(%)</u>	Pore Radius <u>(micron)</u>
395.43	94.73	0.0682	62.35	7.66
478.46	99.04	0.0519	68.30	6.97
561.49	102.22	0.0383	74.29	6.43
658.36	104.86	0.0274	79.94	5.94
715.09	106.03	0.0205	84.14	5.70
832.72	107.79	0.0151	87.68	5.28
957.27	108.64	0.0068	94.00	4.92
1250.00	108.64	0.0000	100.00	0.00

TABLE 35
 PORE SIZE DISTRIBUTION
 SAMPLE NUMBER 5

<u>Fresh</u> <u>Water</u> <u>Injection</u> <u>(cc)</u>	<u>Salt</u> <u>Water</u> <u>Effluent</u> <u>(cc)</u>	<u>$\frac{dR}{dV}$</u>	<u>S</u> <u>(%)</u>	<u>Pore</u> <u>Radius</u> <u>(micron)</u>
6.162	6.162	1.0000	0.00	2.701
6.932	6.929	0.9920	0.09	2.547
7.702	7.680	0.9803	0.23	2.416
8.472	8.423	0.9634	0.45	2.304
9.242	9.138	0.9283	0.97	2.206
13.864	12.982	0.8320	2.51	1.801
16.174	14.683	0.7362	4.82	1.667
19.255	16.827	0.6959	5.95	1.528
23.876	19.822	0.6481	7.55	1.372
30.038	23.371	0.5760	10.53	1.224
35.429	26.088	0.5040	14.29	1.127
40.050	28.158	0.4479	17.73	1.060
46.212	30.623	0.4001	21.06	0.986
53.144	33.091	0.3560	24.59	0.920
62.386	36.085	0.3241	27.54	0.849
73.939	39.320	0.2800	32.31	0.780
87.803	42.426	0.2240	39.50	0.716

(Continued)

TABLE 35
 PORE SIZE DISTRIBUTION
 SAMPLE NUMBER 5

Fresh Water Injection <u>(cc)</u>	Salt Water Effluent <u>(cc)</u>	$\frac{dR}{dV}$ <u> </u>	S <u>(%)</u>	Pore Radius <u>(micron)</u>
100.896	44.939	0.1920	44.37	0.668
120.921	48.144	0.1600	49.98	0.610
134.014	49.924	0.1360	55.01	0.579
150.959	51.958	0.1200	58.74	0.546
163.282	53.239	0.1040	62.92	0.525
183.307	54.841	0.0800	69.73	0.495
201.022	55.691	0.0480	79.91	0.473
229.519	56.603	0.0320	85.49	0.443
274.961	57.330	0.0160	91.86	0.404
347.359	57.620	0.0040	97.59	0.360
429.000	57.620	0.0000	100.00	0.000

TABLE 36
 PORE SIZE DISTRIBUTION
 SAMPLE NUMBER 6

<u>Fresh</u> <u>Water</u> <u>Injection</u> <u>(cc)</u>	<u>Salt</u> <u>Water</u> <u>Effluent</u> <u>(cc)</u>	<u>$\frac{dR}{dV}$</u>	<u>S</u> <u>(%)</u>	<u>Pore</u> <u>Radius</u> <u>(micron)</u>
22.251	22.25	1.0000	0.00	34.83
33.377	33.03	0.9690	0.54	28.44
44.503	42.69	0.8683	3.19	24.63
55.628	50.71	0.7209	8.35	22.03
66.754	57.09	0.5734	14.81	20.11
77.880	62.27	0.4647	20.54	18.62
89.005	66.67	0.3948	24.78	17.42
100.131	70.38	0.3335	29.13	16.42
111.257	73.57	0.2867	32.81	15.58
122.383	76.41	0.2562	35.48	14.85
144.634	81.24	0.2171	41.37	13.66
166.885	85.21	0.1784	43.65	12.72
200.262	90.13	0.1474	47.72	11.61
255.891	96.60	0.1163	52.63	10.27
300.393	100.73	0.0930	57.31	9.48
344.896	104.18	0.0775	60.98	8.85
389.400	106.94	0.0620	65.19	8.33

(Continued)

TABLE 36
 PORE SIZE DISTRIBUTION
 SAMPLE NUMBER 6

Fresh Water Injection <u>(cc)</u>	Salt Water Effluent <u>(cc)</u>	$\frac{dR}{dV}$ <u> </u>	S <u>(%)</u>	Pore Radius <u>(micron)</u>
522.907	113.15	0.0465	69.94	7.19
689.792	118.33	0.0310	76.35	6.26
1190.448	126.09	0.0155	84.75	4.76
1412.962	126.95	0.0039	95.66	4.37
2300.000	126.95	0.0000	100.00	0.00

TABLE 37
 PORE SIZE DISTRIBUTION
 SAMPLE NUMBER 7

<u>Fresh</u> <u>Water</u> <u>Injection</u> <u>(cc)</u>	<u>Salt</u> <u>Water</u> <u>Effluent</u> <u>(cc)</u>	<u>$\frac{dR}{dV}$</u>	<u>S</u> <u>(%)</u>	<u>Pore</u> <u>Radius</u> <u>(micron)</u>
27.237	27.237	1.0000	0.00	36.22
32.872	32.759	0.9799	0.46	32.97
38.507	37.966	0.9240	2.01	30.46
46.021	44.218	0.8320	4.92	27.86
53.534	49.687	0.7280	9.03	25.86
62.926	55.623	0.6320	13.37	23.83
70.440	59.770	0.5519	17.62	22.52
81.710	65.180	0.4800	21.89	20.91
92.980	69.779	0.4080	26.85	19.60
108.008	74.948	0.3440	31.87	18.19
134.305	82.101	0.2720	38.42	16.31
156.846	86.789	0.2080	45.67	15.09
183.143	91.207	0.1680	50.96	13.97
241.374	98.661	0.1280	57.14	12.17
314.631	105.107	0.0880	65.28	10.66
436.726	111.945	0.0560	73.77	9.05
549.430	115.551	0.0320	82.60	8.06

(Continued)

TABLE 37
 PORE SIZE DISTRIBUTION
 SAMPLE NUMBER 7

Fresh Water Injection <u>(cc)</u>	Salt Water Effluent <u>(cc)</u>	$\frac{dR}{dV}$ <u> </u>	S <u>(%)</u>	Pore Radius <u>(micron)</u>
709.093	118.106	0.0160	90.01	7.10
831.189	118.594	0.0040	97.20	6.56
865.000	118.594	0.0000	100.00	0.00

TABLE 38
PORE SIZE DISTRIBUTION
SAMPLE NUMBER 8

Fresh Water Injection <u>(cc)</u>	Salt Water Effluent <u>(cc)</u>	$\frac{dR}{dV}$ <u> </u>	S <u>(%)</u>	Pore Radius <u>(micron)</u>
13.538	13.538	1.0000	0.00	7.373
18.615	18.509	0.9789	0.18	6.288
23.692	23.195	0.9230	0.85	5.574
30.462	28.876	0.8391	2.11	4.916
37.231	33.893	0.7413	4.01	4.446
44.000	38.296	0.6503	6.17	4.090
50.769	42.178	0.5735	8.32	3.808
57.538	45.633	0.5105	10.35	3.577
64.308	48.757	0.4615	12.15	3.383
74.462	53.018	0.4195	13.87	3.144
82.923	56.272	0.3846	15.53	2.979
93.077	59.893	0.3566	17.07	2.812
103.231	63.231	0.3286	18.67	2.670
118.462	67.811	0.3007	20.50	2.493
133.692	71.964	0.2727	22.61	2.346
157.385	77.763	0.2448	24.99	2.163
187.846	84.367	0.2168	27.80	1.979

(Continued)

TABLE 38
 PORE SIZE DISTRIBUTION
 SAMPLE NUMBER 8

Fresh Water Injection <u>(cc)</u>	Salt Water Effluent <u>(cc)</u>	$\frac{dR}{dV}$ <u> </u>	S <u>(%)</u>	Pore Radius <u>(micron)</u>
231.846	92.675	0.1888	31.15	1.782
296.154	103.018	0.1608	35.28	1.571
389.231	115.385	0.1329	40.55	1.375
558.462	133.136	0.1049	47.49	1.118
719.231	145.503	0.0769	57.44	1.012
880.000	153.373	0.0490	70.25	0.915
1040.769	156.746	0.0210	85.93	0.841
1106.789	156.977	0.0035	97.53	0.815
1300.000	156.977	0.0000	100.00	0.000

TABLE 39
 PORE SIZE DISTRIBUTION
 SAMPLE 9

Fresh Water Injection <u>(cc)</u>	Salt Water Effluent <u>(cc)</u>	$\frac{dR}{dV}$ <u> </u>	S <u>(%)</u>	Pore Radius <u>(micron)</u>
6.629	6.629	1.0000	0.00	3.261
8.287	8.242	0.9733	0.19	2.917
9.944	9.720	0.8918	0.94	2.663
14.916	13.517	0.7657	2.32	2.174
19.888	16.663	0.6305	4.53	1.883
24.860	19.350	0.5406	6.50	1.684
31.489	22.516	0.4774	8.23	1.496
39.775	26.024	0.4235	10.10	1.331
48.062	29.160	0.3783	12.07	1.211
56.349	31.997	0.3424	13.97	1.119
69.607	36.058	0.3063	16.21	1.006
81.208	39.193	0.2702	18.97	0.932
96.124	42.286	0.2342	22.18	0.856
107.725	45.091	0.2072	25.04	0.809
119.326	47.286	0.1892	27.02	0.769
140.871	50.974	0.1712	29.54	0.707
180.647	57.065	0.1532	32.33	0.625
201.192	59.977	0.1352	35.92	0.592

(Continued)

TABLE 39
 PORE SIZE DISTRIBUTION
 SAMPLE 9

Fresh Water Injection <u>(cc)</u>	Salt Water Effluent <u>(cc)</u>	$\frac{dR}{dV}$ <u> </u>	S <u>(%)</u>	Pore Radius <u>(micron)</u>
227.052	62.888	0.1171	39.93	0.557
263.513	66.501	0.0991	44.42	0.517
341.406	72.817	0.0811	49.64	0.454
455.761	80.029	0.0631	56.40	0.393
576.744	85.478	0.0450	65.43	0.350
732.532	89.689	0.0270	76.87	0.310
870.089	90.928	0.0090	91.37	0.285
1122.000	90.928	0.0000	100.00	0.000

TABLE 40
 PORE SIZE DISTRIBUTION
 SAMPLE NUMBER 10

<u>Fresh</u> <u>Water</u> <u>Injection</u> <u>(cc)</u>	<u>Salt</u> <u>Water</u> <u>Effluent</u> <u>(cc)</u>	<u>$\frac{dR}{dV}$</u>	<u>S</u> <u>(%)</u>	<u>Pore</u> <u>Radius</u> <u>(micron)</u>
0.943	0.943	1.0000	0.00	22.99
3.773	3.504	0.9051	0.11	11.49
7.545	6.074	0.6812	1.11	8.13
11.318	7.895	0.4827	2.90	6.37
15.091	9.294	0.3708	4.41	5.75
18.865	10.432	0.3016	5.66	5.14
24.523	11.895	0.2587	6.62	4.51
32.068	13.619	0.2285	7.51	3.95
47.159	16.676	0.2026	8.50	3.25
73.568	21.457	0.1810	9.71	2.60
158.455	35.361	0.1638	11.22	1.77
203.727	41.996	0.1466	14.48	1.56
284.841	52.485	0.1293	18.67	1.32
341.432	58.827	0.1121	24.35	1.21
415.000	65.803	0.0948	31.55	1.10
491.829	71.764	0.0776	40.09	1.01
574.146	76.731	0.0603	50.21	0.932

(Continued)

TABLE 40
 PORE SIZE DISTRIBUTION
 SAMPLE NUMBER 10

Fresh Water Injection <u>(cc)</u>	Salt Water Effluent <u>(cc)</u>	$\frac{dR}{dV}$ <u> </u>	S <u>(%)</u>	Pore Radius <u>(micron)</u>
661.951	80.516	0.0431	62.01	0.868
755.244	82.929	0.0259	75.62	0.812
859.512	83.828	0.0086	91.16	0.762
1000.000	83.828	0.0000	100.00	0.000

TABLE 41
 PORE SIZE DISTRIBUTION
 20 - 40 MESH SANDPACK

Fresh Water Injection <u>(cc)</u>	Salt Water Effluent <u>(cc)</u>	$\frac{dR}{dV}$ <u> </u>	S <u>(%)</u>	Pore Radius <u>(micron)</u>
76.392	76.392	1.0000	0.00	27.25
85.842	85.479	0.9615	2.86	25.72
90.568	89.586	0.8694	10.56	25.03
95.293	93.112	0.7462	21.43	24.40
100.018	95.947	0.6000	35.00	23.82
104.744	98.092	0.4539	49.22	23.28
109.469	99.655	0.3308	61.78	22.76
115.769	101.060	0.2230	73.27	22.14
123.645	102.030	0.1230	84.54	21.42
131.520	102.454	0.0538	92.87	20.77
147.271	102.696	0.0154	97.80	19.63
215.000	102.696	0.0000	100.00	0.00

TABLE 42
MISCIBLE DISPLACEMENT
IN
TURBULENT FLOW REGIME
SAMPLE 2

Fresh Water Injection <u>(cc)</u>	Salt Water Effluent <u>(cc)</u>
50.662	50.66
70.927	68.75
91.192	82.91
111.457	94.03
131.722	103.18
151.987	111.24
172.252	118.43
212.782	130.63
253.312	140.66
303.975	151.01
374.902	162.82
425.565	169.64
516.757	179.44
587.685	185.93
689.009	194.10

(Continued)

TABLE 42
MISCIBLE DISPLACEMENT
IN
TURBULENT FLOW REGIME
SAMPLE 2

Fresh Water Injection <u>(cc)</u>	Salt Water Effluent <u>(cc)</u>
790.334	199.54
891.659	204.45
1398.284	223.51
1702.259	231.69
2515.858	240.40
2867.495	242.31
3212.000	242.31

BIBLIOGRAPHY

1. Valore, Rudoph C., Cellular Concretes, Composition and Methods of Preparation: Journal of the American Concrete Institute, May 1954, Proc. V. 50, P. 773-796.
2. _____, Cellular Concretes, Physical Properties: ACI Journal, June 1954, Poc. V. 50, P. 817-836.
3. Suleimanof, A. B., et al, Experimental Commercial Scale Use of Foam Cement for Consolidating the Well Bottom Zone: (Translation from Russian), Source unknown.
4. Aspdin, Joseph, An Improvement in the Modes of Producing Artificial Stone: British Patent No. 5022 (1824).
5. Halliburton Services, Halliburton Cementing Tables: Duncan, Oklahoma, Section No. 230 (1972).
6. Craft, B. C., Holden, R. H., and Graves, E. D., Well Design: Drilling and Production: Englewood Cliffs, New Jersey, Prentice-Hall, Inc., p. 158-244 (1962).
7. API RP - 10B: Testing Oil Well Cements and Cement Additives: Dallas, Texas (1972).
8. API RP - 13B: Standard Procedure for Testing Drilling Fluid, April, 1969.
9. Coleman, J. R., and Carrigan, G. L., Fineness and Water Cement Ratio in Relation of Volume and Permeability of Cement: Trans. AIME, V. 142, p. 205-215 (1941).
10. Sanders, Paul A., Principles of Aerosol Technology: New York, New York, Van Nostrand Reinhold Co., p. 210-221 (1970).
11. Shaw, D. J., Introduction to Colloid and Surface Chemistry: London, England, Butterworth and Co., P. 167-218 (1970).
12. Bikerman, J. J., Foams: N.Y., N.Y., Van Nostrand Reinhold Co., (1941).
13. Bancroft, Wilder, D., Applied Colloid Chemistry: N.Y., N.Y., McGraw-Hill Book Co., Inc., p. 268-273 (1921).

14. Stable Foam Circulating Fluid: World Oil, November 1966, v. 163, no. 6, p. 82-90.
15. Hutchinson, S. D., Foam Workovers Cut Costs 50%: World Oil, November, 1969, p. 73-94.
16. Blauer, R. E., and Kohlhaas, C. A., Formation Fracturing with Foam: SPE 5003, presented at 49th Annual Fall Meeting SPE of AIME, Houston, Texas (October 6-9, 1974).
17. Raza, S. H., Foam in Porous Media: Characteristics and Potential Applications: SPEJ, Dec. 1970, p. 328-336.
18. Al-Attar, Hazim H., The Evaluation of Oil Foam for Use as a Displacing Medium for Oil Recovery in Porous Media: PhD Thesis, Colorado School of Mines, Golden, Colo. (1976).
19. Abbott, W. A., An Analysis of Slip Velocities of Spherical Particles in Foam Drilling Fluid: MS Thesis, Colorado School of Mines, Golden, Colo. (1974).
20. King, George E., Factors Affecting Dynamic Fluid Leakoff with Foam Fracturing Fluids: SPE 6817, presented at 52nd Annual Fall Meeting of SPE of AIME, Denver, Colorado, Oct. 9-12, 1976.
21. Aldrich, C. S., Strength, Permeability and Porosity of a Cellular Oil Well Cement: MS Thesis, Colorado School of Mines, Golden (1974).
22. Slattery, Joseph P., Compressive and Tensile Strengths of Foam Cement with Common Additives: MS Thesis, Colorado School of Mines, Golden (1976).
23. Al-Mashat, Ali M., Rheology of Foam Cement: PhD Thesis, Colorado School of Mines, Golden (1976).
24. Aylsworth, Jonas W., and Dyer, Frank L., U. S. Patent 1,087,098 (1914).
25. Bayer, Eric Christian, German Patent 421,777 (1923).
26. Bass, D. M., and Aldrich, C. S., Personal Communications: Petroleum Engineering Department, Colorado School of Mines.
27. Klinkenberg, L. J., Pore Size Distribution of Porous Media and Displacement Experiments with Miscible Fluids: Trans. AIME, v. 210, p. 366-369 (1957).

28. Detkov, V. P., and Sabrizyanov, A. K., The Use of Aerated Plugging Suspensions for Well Cementations: (in Russian) Neftyanoe Khozyaistov, No. 5, May 1976, p. 16-20.
29. Danyushevsky, V. S., et al, The Possible Use of Surfactant Based Foam Cements for Well Cementing: (in Russian) Neftyanoe Khozyaistov, No. 7, October 1976, p. 48-50.
30. Dumbauld, G. K., et al, A Lightweight, Low Water Loss, Oil-Emulsion Cement for Use in Oil Wells: Trans. AIME, v. 207, p. 99-104 (1956).
31. Howard, George C., and Scott, P. P., Plugging Off Water in Fractured Formations: Trans. AIME, v. 201, p. 132-137 (1954).
32. Coffey, H. F., and Clark, R. C., Jr., A Ten Pound Cement Slurry for Oil Wells: Trans. AIME, v. 201, p. 146-148 (1954).
33. Amyx, J. W., Bass, D. M., and Whiting, R. L., Petroleum Reservoir Engineering: New York, New York, McGraw-Hill, Inc., p. 36-129 (1960).
34. Timoshenko, S. P., and Goodier, J. N., Theory of Elasticity: New York, New York, McGraw-Hill Book Company, p. 392-398 (1970).
35. Handbook of Chemistry and Physics: Cleveland, Ohio, The Chemical Rubber Publishing Co., 44th Edition (1962).

APPENDIX
TEST SEQUENCE AND CALCULATIONS
SAMPLES OF SET CEMENT

1. Approximately 450 cc of foam was generated by mixing 50 cc of water with 0.10 to 0.20 cc Adofoam BF-1 in a high speed blender.
2. Dry cement was sifted through a U. S. Standard 40 Mesh Screen and weighed. The dry cement was then mixed with water in a blender. The volume of mix-water was calculated as follows:

$$\text{Mix-Water} = (0.44 \text{ cc/gm})(\text{gms of Dry Cement}) - (50 \text{ cc}) \quad (\text{A-1})$$

3. The cement slurry mixed in Step 2 was blended with the foam of Step 1 until a consistent foam cement slurry was obtained.
4. The bulk volume of a Lucite tube was measured by weight as follows:

$$\text{Bulk Volume} = \frac{(\text{Weight filled with Water}) - (\text{Dry Weight of Tube})}{(\text{Density of Water})} \quad (\text{A-2})$$

The bulk volume was also calculated from the tube dimensions and by volumetric measurement. Determination by weight proved to be the most precise measurement of volume.

5. The foam cement slurry created in Step 3 was placed in the Lucite tube and the tube was sealed. The weight was recorded and the weight of the sample calculated as follows:

$$\text{Sample Weight} = (\text{Weight of Tube \& Sample}) - (\text{Dry Weight of Tube}) \quad (\text{A-3})$$

The predicted quality of the foam cement sample was determined from the sample weight and the bulk volume (measured in Step 4).

$$\text{Predicted Quality} = 100\% - \frac{(8.33)(100\%)(\text{Sample Weight})}{(15.8)(\text{Bulk Volume})} \quad (\text{A-4})$$

6. The sample was allowed to set for 72 hours. Valves were then installed in the Lucite tube and the weight was recorded. This weight will be referred to as the initial weight of the sample.
7. A vacuum was placed on the system for several hours to reduce the air content of the sample. The sample was then saturated with water. The sample was considered to be completely saturated with water when the sample weight at 25 psig was the same as the weight at atmospheric pressure. The measured quality was then determined as follows:

$$\text{Measured Quality} = \frac{(\text{Saturated Sample Weight}) - (\text{Initial Weight})}{(\text{Bulk Volume})(\text{Density of Saturating Fluid})} \quad (\text{A-5})$$

8. The rate of flow was measured at various differential pressures. Initially, this differential pressure was small and was increased in increments to a maximum of 25 psig. The sample weight at 25 psig was then recorded. Flow rates were then measured at a differential pressure of 25 psig followed by decreasing increments of differential pressure. The weight of the sample at atmospheric pressure was then recorded. The presence of air in the sample could readily be detected by the recorded weights as well as a variation in flow rate between the first and second tests.
9. Samples were allowed to set 24 hours and Step 8 was then repeated. Flow tests were conducted a minimum of three times on any sample. When the recorded weights were the same, the flow rates did not vary significantly between tests.
10. Rate of Flow was plotted versus differential pressure. Permeability was calculated from the slope of the linear portion of the curve using Darcy's Law.
11. The fresh water contained in the sample was displaced by a dilute solution of NaCl. These tests were conducted in the darcian flow regime, generally at a differential pressure of 1 to 2 psi. The conductivity of the effluent was monitored continuously and the total volume of effluent was measured. The relative volumes of fresh water and

salt solution were calculated from their conductivities and that of the effluent. Calculation of pore size and distribution was obtained from equations (9) and (10) in the text. The displaced porosity was calculated from the total volume of fresh water in the effluent.

$$\text{Displaced Porosity} = \frac{(\text{Volume of Fresh Water Displaced})}{(\text{Bulk Volume of Sample})} \quad (\text{A-6})$$

12. Differential pressure was increased to 25 psi and the salt solution displaced additional fresh water.
13. Step 11 was repeated with fresh water displacing the salt solution.
14. Additional displacement tests were run on selected samples. Differential pressure was varied and the pore size, distribution and displaced pore volume were calculated for each test. Calculated values were similar within the darcian flow regime while a large variation in values was obtained at higher differential pressures.
15. The sample was dried with compressed air which had been passed through a dessicant (silica gel). The air flow rate was monitored and the sample was considered to be dry when the rate stabilized. The sample was weighed and the total porosity was calculated.

$$\text{Total Porosity} = \frac{(\text{Saturated Sample Weight}) - (\text{Dry Sample Weight})}{(\text{Bulk Volume}) (\text{Density of Water})} \quad (\text{A-7})$$

The initial water saturation was then calculated from the total porosity and the initial and dry sample weights.

$$\text{Water Saturation} = \frac{(\text{Initial Sample Weight}) - (\text{Dry Sample Weight})}{(\text{Total Porosity}) (\text{Density of Water})}$$

(A-8)